2004 ASME Rayleigh Lecture

Fluid-Structure Interaction and Acoustics

Hafiz M. Atassi

University of Notre Dame

"Rarely does one find a mass of analysis without illustrations from experience."

Rayleigh

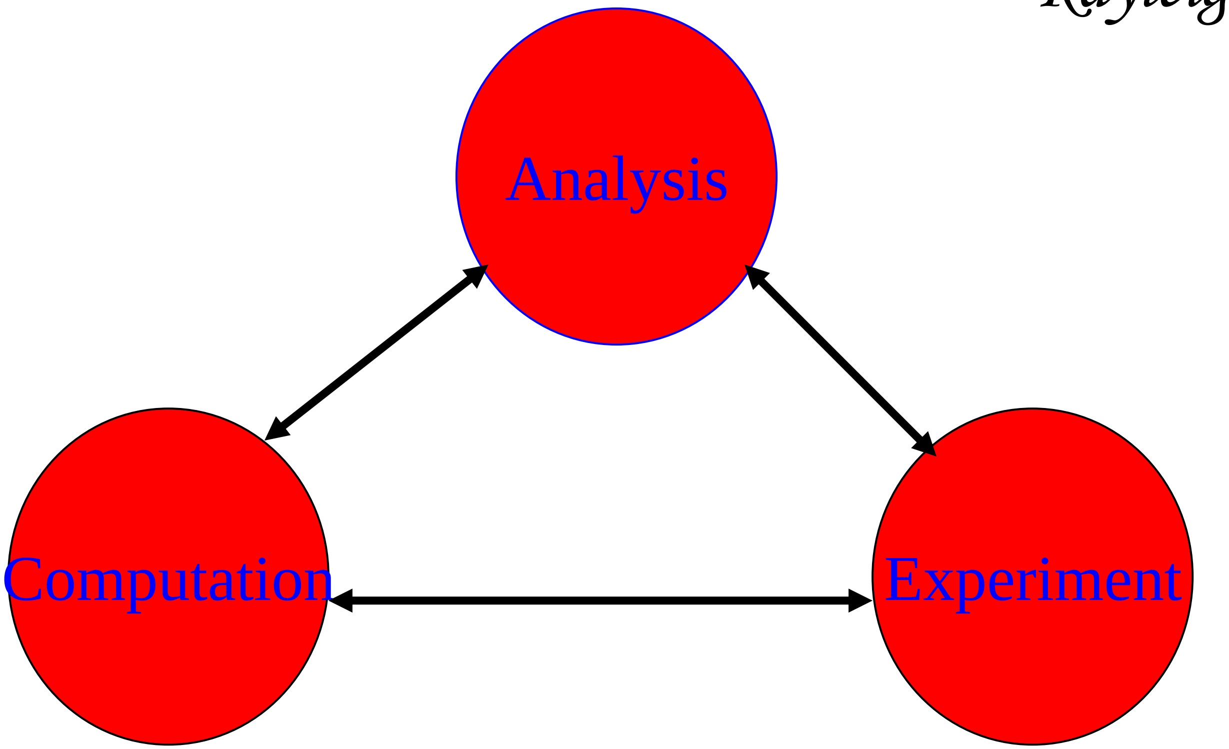

Overview of Lecture

- Sound Generated by Fluid-Structure Interaction Phenomena
- Linear Acoustic, Entropic and Vortical Mode Splitting
- Non-uniform Flow Effects
- Application:
  - Aircraft Turbofan Interaction Noise
  - Marine Propellers with Elastic Ducts
- Conclusions

Acknowledgements

Research Funding past 5 Years

- Office of Naval Research
- NASA Glenn Research Center
- Ohio Aerospace Institute Aeroacoustic Consortium
- Center for Applied Mathematics, University of Notre Dame
- National Science Foundation
- Pratt & Whitney
- Air Force Office of Scientific Research

Students and Associates

- Jisheng Fang
- James Scott
- Sheryl Patrick Grace
- Vladimir Golubev
- Pascal Ferrand
- Romeo Susan-Resiga
- Amr Ali
- Basman Elhadidi
- Igor Vinogradov
- Dan Monahan
- Wenglan Zhang
- Michaela Logue

When Acoustics is Important?

- High Speed
  - Aeronautics
  - Transportation
  - Energy Production
- Stealth
  - Submarines
- Structural Damage
- High Perceived Noise Level
  - Frequency Range
  - Intensity

Generic Problem
Airfoil in Nonuniform Flow

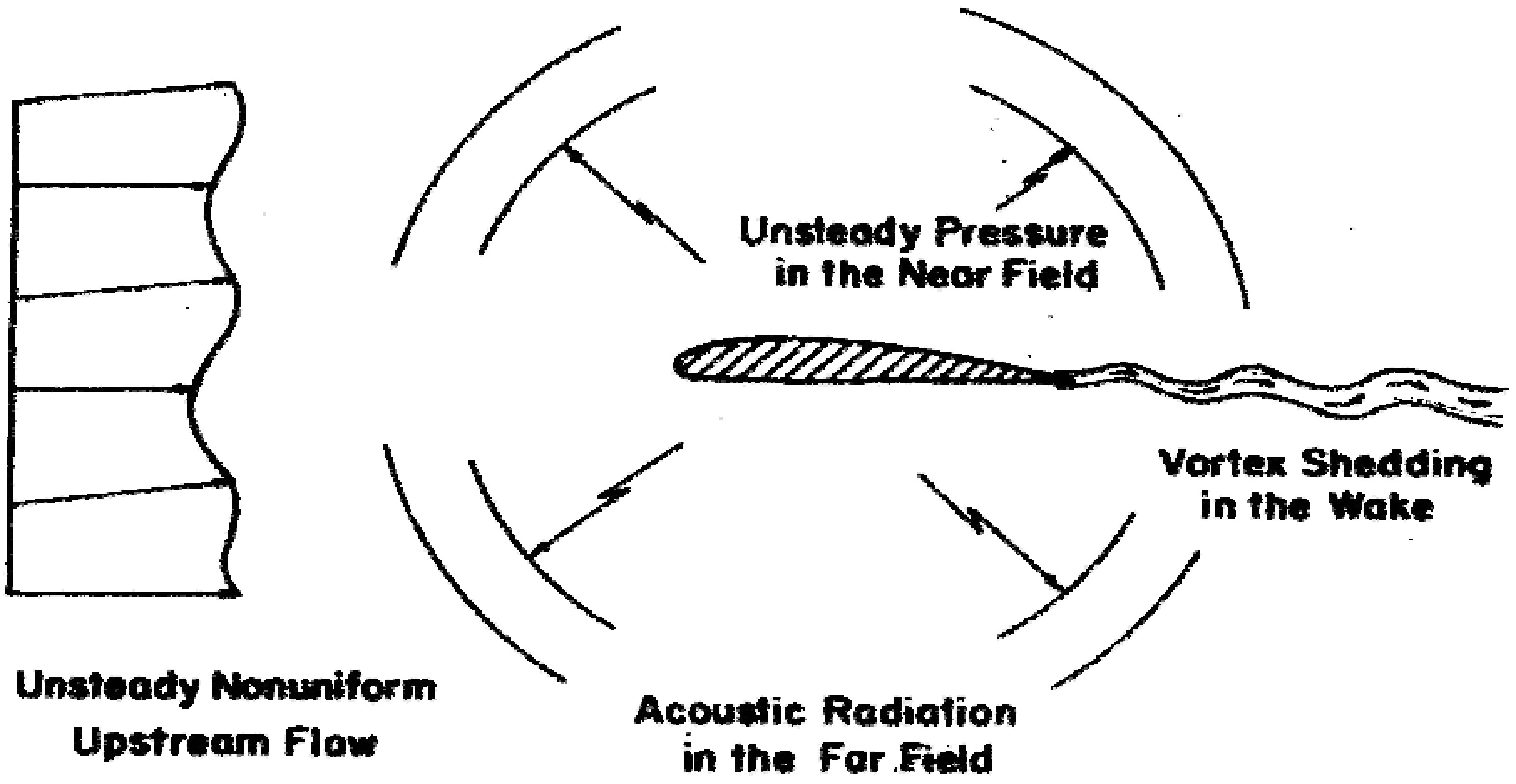

Aeroacoustics and Unsteady Aerodynamics

- Lighthill's acoustic analogy.
- Sound is the far-field signature of the unsteady flow.
- The aeroacoustic problem is similar to that of forced vibration but with emphasis on the far-field. It is a much more difficult computational problem whose outcome depends on preserving the far-field wave form with minimum dispersion and dissipation.
- Inflow/outflow nonreflecting boundary conditions must be derived to complete the mathematical formulation as a substitute for physical causality.

Kovasnay Modes
(1953)

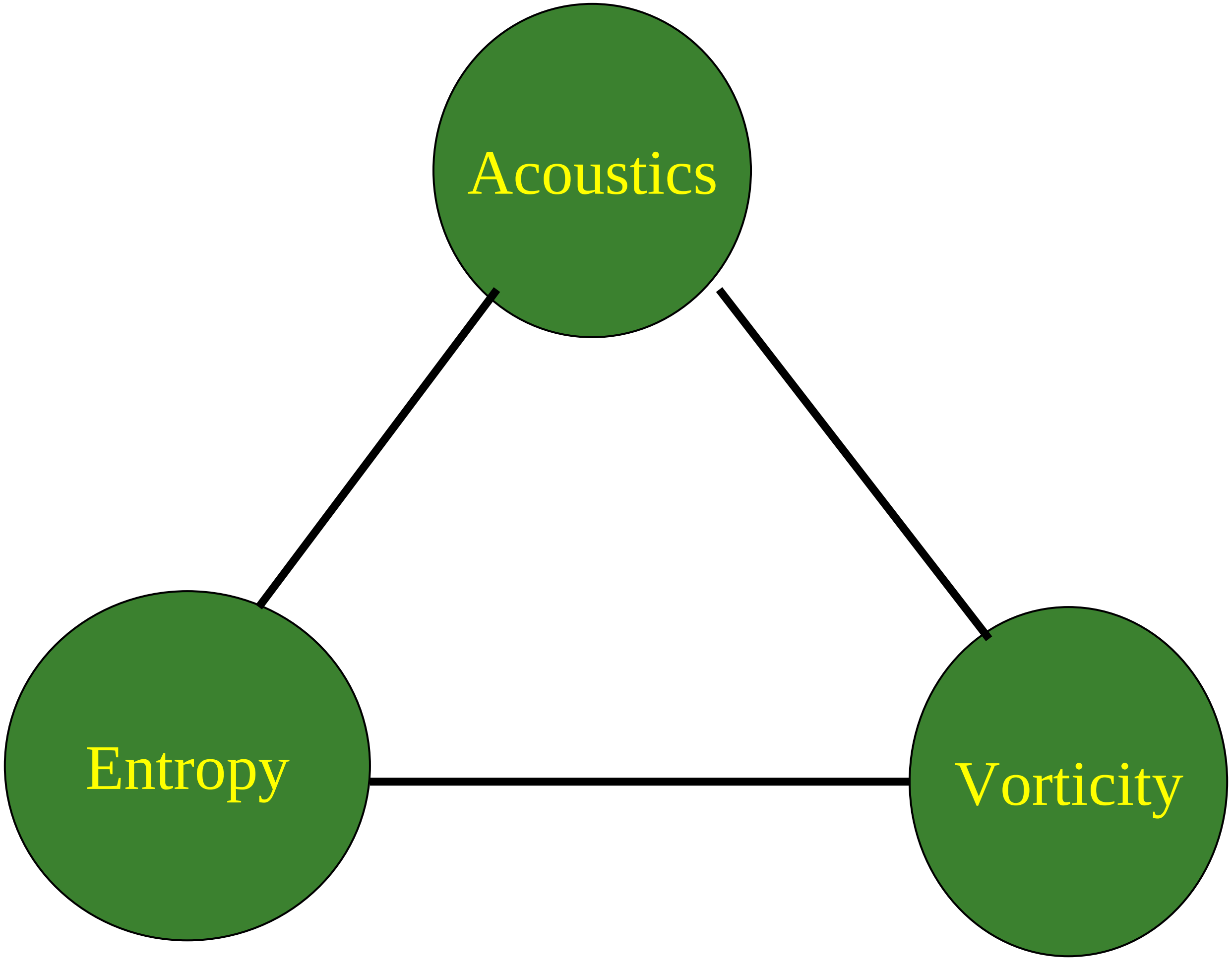

Splitting Theorem for Uniform flow

$$\mathbf{V}(\mathbf{x},t) = \mathbf{U} + \mathbf{u}(\mathbf{x},t)$$

$$\mathbf{u} = \mathbf{u}^{(R)} + \nabla\Phi$$

$$\frac{D_0 \mathbf{u}^{(R)}}{Dt} = 0$$

$$\frac{D_0 s'}{Dt} = 0$$

$$\left(\frac{D_0{}^2}{Dt^2} - c_0^2 \nabla^2 \right)\Phi = 0$$

$$\frac{D_0}{Dt} \equiv \frac{\partial}{\partial t} + \mathbf{U}\cdot\nabla$$

Disturbances in Uniform Flows

Splitting Theorem:

The flow disturbances can be split into distinct potential (acoustic), vortical and entropic modes obeying three independent equation:

- The vortical velocity is solenoidal, purely convected and completely decoupled from the pressure fluctuation
- The potential (acoustic) velocity is directly related to the pressure fluctuations.
- The entropy is purely convected and only affects the density through the equation of state.
- Coupling between the vortical and potential velocity occurs only along the body surface.
- Upstream conditions can be specified independently for various disturbances.

Equations for Linear Aerodynamics

- Vortical Mode: $\vec{u}_v = \vec{u}_\infty(\vec{x} - \vec{U}i)$
  - Harmonic Component

$$\vec{u}_g = \vec{a}e^{i(\vec{k}\cdot\vec{x} - \omega t)}$$

- Potential Mode:

$$\left(\frac{1}{c_0^2}\frac{D_0^2}{Dt^2} - \nabla^2\right)\phi = 0$$

- Boundary Conditions: impermeability along blade surface, Kutta condition at trailing edge, allow for wake shedding in response to gust.

Issues Associated with Nonuniform Flows

- Linear vs Nonlinear Analysis:
  - Uniform mean flow, RDT, fully nonlinear.
- Inflow Disturbance Description:
  - Can we consider separately acoustic, vortical and entropic disturbances?
- What are the upstream boundary conditions to be specified?
- What are the conditions for flow instability?
- What is the effect of high frequency?
  - Can we still apply The Kutta condition?
  - Difficult computational issues but help from asymptotics?
- What are transonic flow effects?
- Conservation relations for acoustic intensity and power?
- Turbulence modification.
- Coupling with structural modes.

Linear Versus Nonlinear

Mode Interaction and Coupling

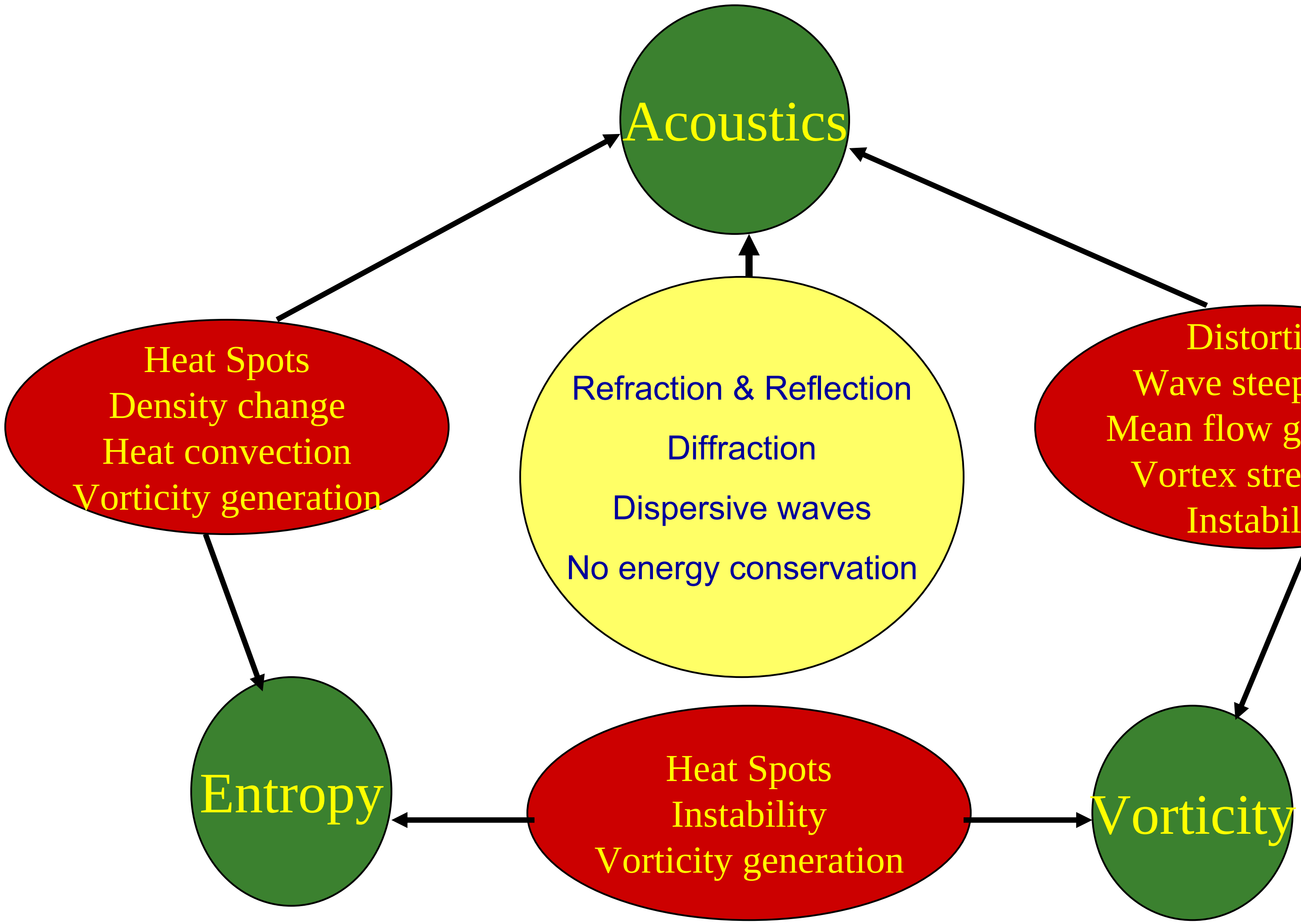

Vortex Traveling around an airfoil

Linear Theory

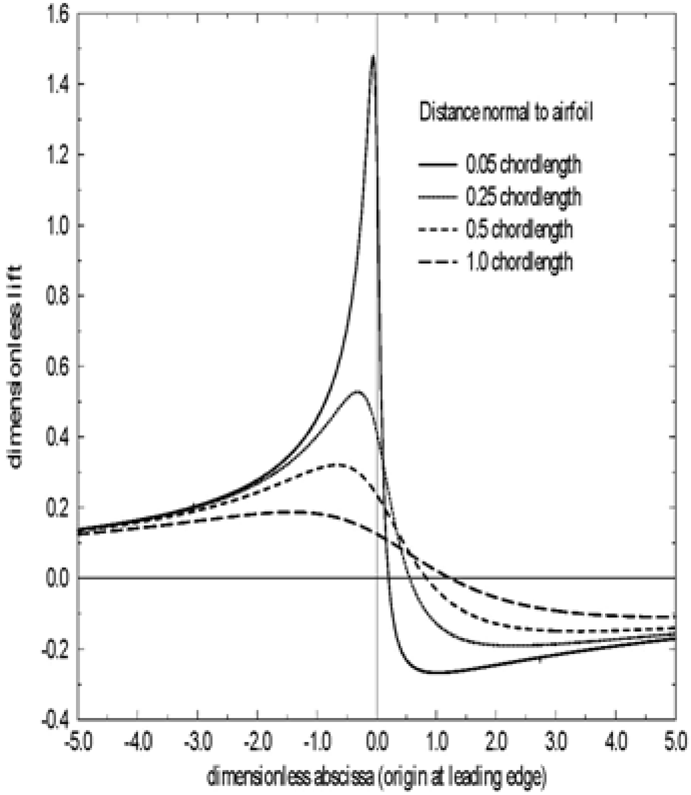

Comparison Between Theory and Computation:

Surface Pressure Induced By the Motion of a Vortex Near the Trailing Edge

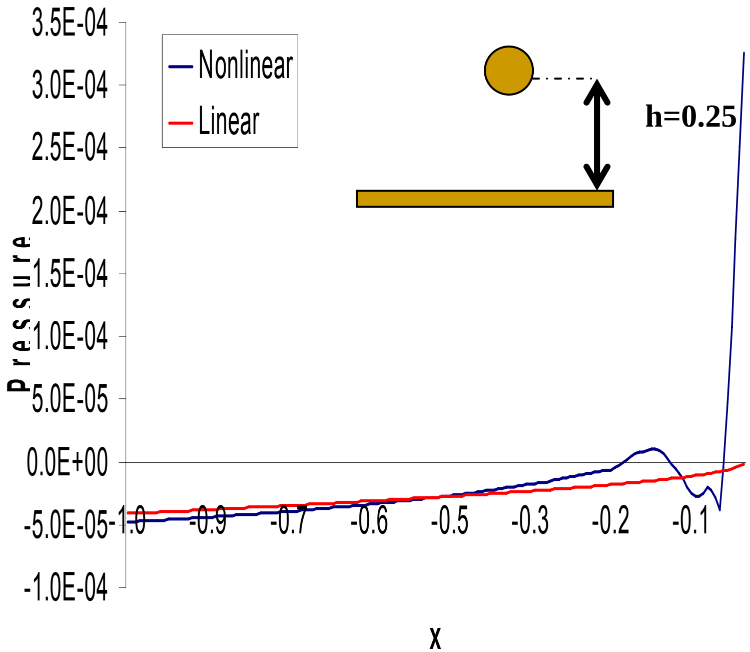

Vortex in a Strongly Nonuniform Flow at Low Mach Number

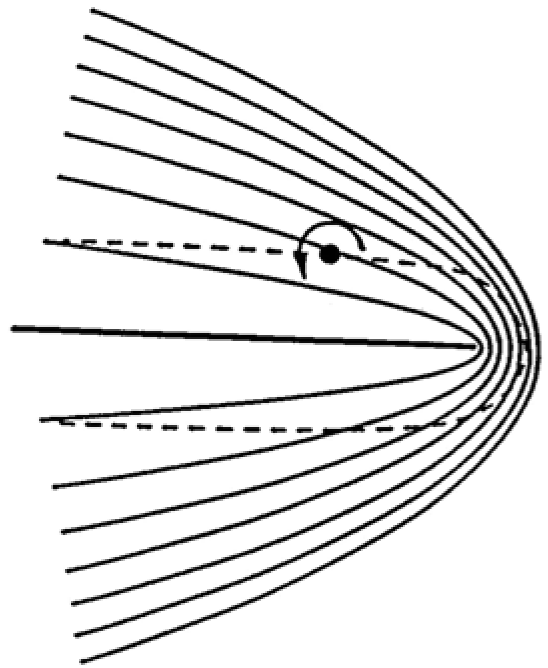

As the vortex travels near the trailing edge it is no longer convected by the mean flow. Its trajectory crosses the undisturbed mean flow. This increases the amount of fluid energy converted into acoustic energy. The acoustic power scales with M^3, much higher than that predicted by a dipole (M^6).

Cascade Flow with local Regions of Strong Interaction

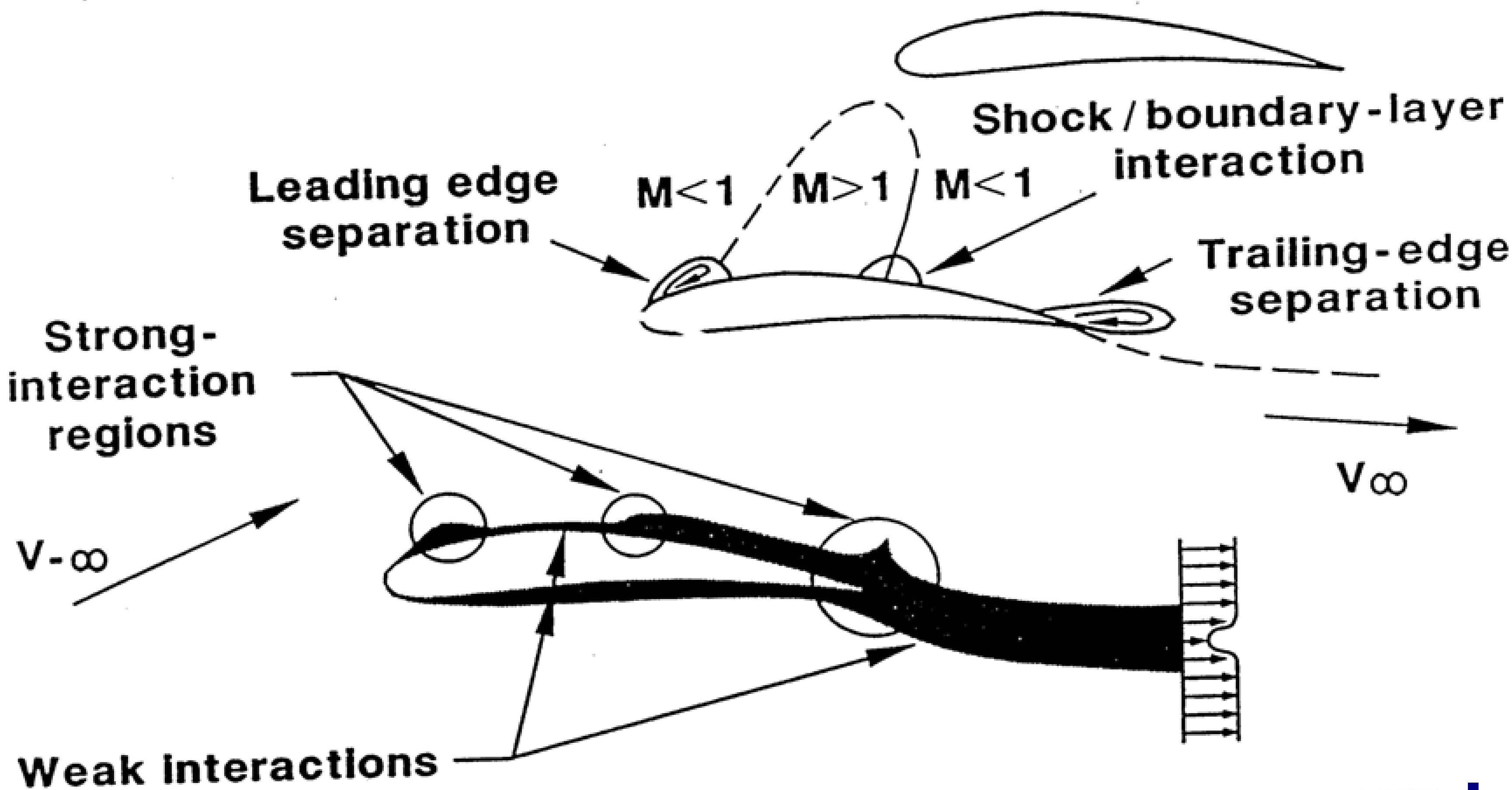

VORTEX STRETCHING AT THE STAGNATION POINT

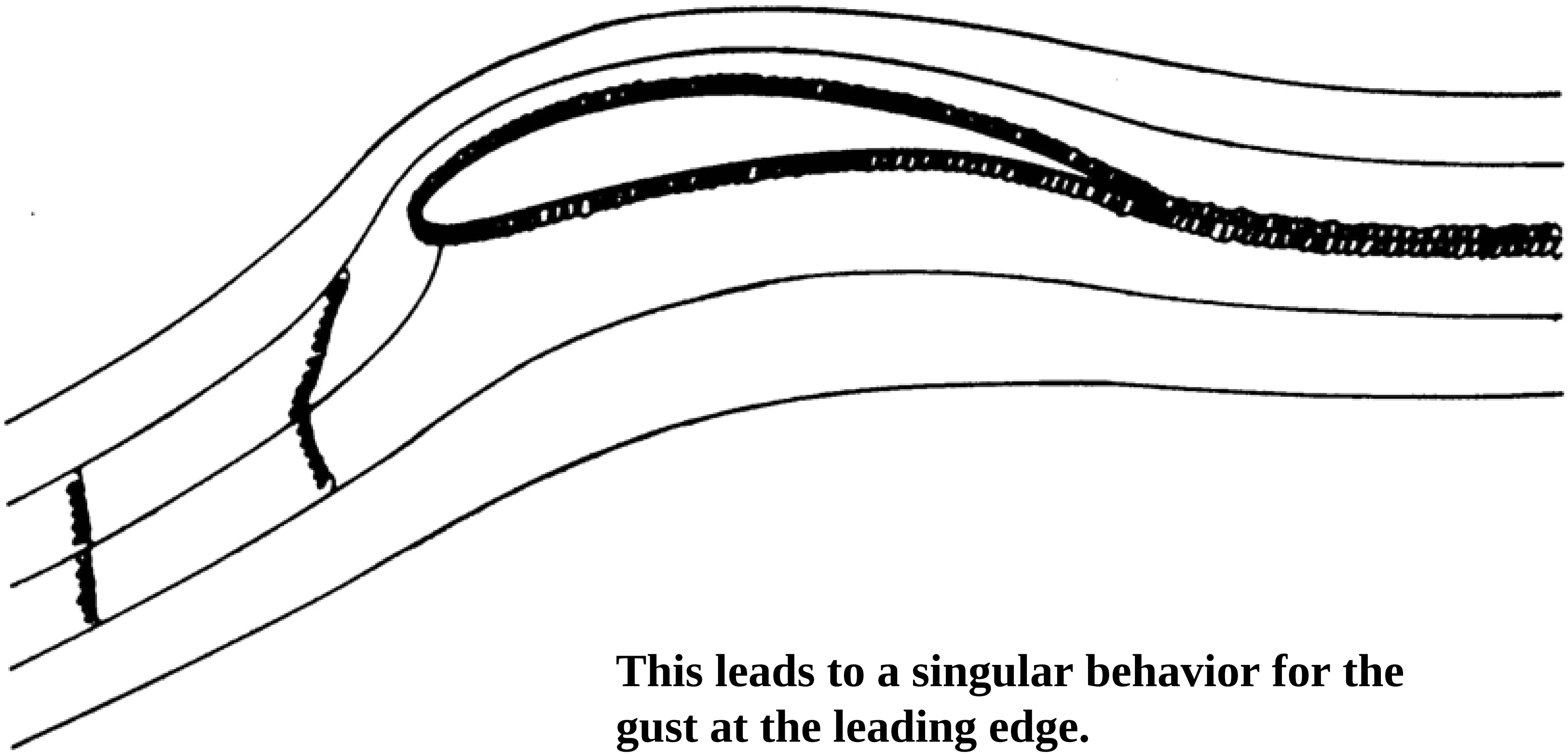

This leads to a singular behavior for the gust at the leading edge.

Comparison between Linear and Nonlinear Analyses for Subsonic Flows

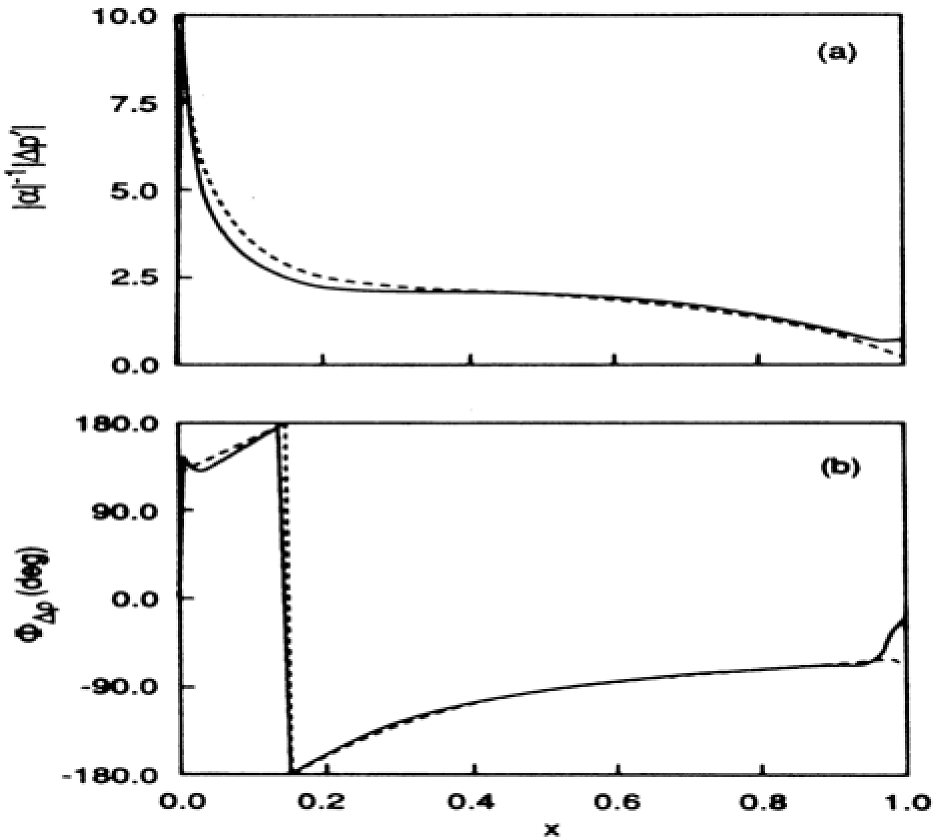

Magnitude (a) and Phase (b) of the first Harmonic Unsteady Pressure Difference Distribution for the subsonic Cascade Underhoing an In-Phase Torsional Oscillation of Amplitude a=2o at k1=0.5 about Midchord; M=0.7;

______ , Linear Analysis; ……, Nonlinear Analysis.

Comparison between Linear and Nonlinear Analyses for Transonic Flows

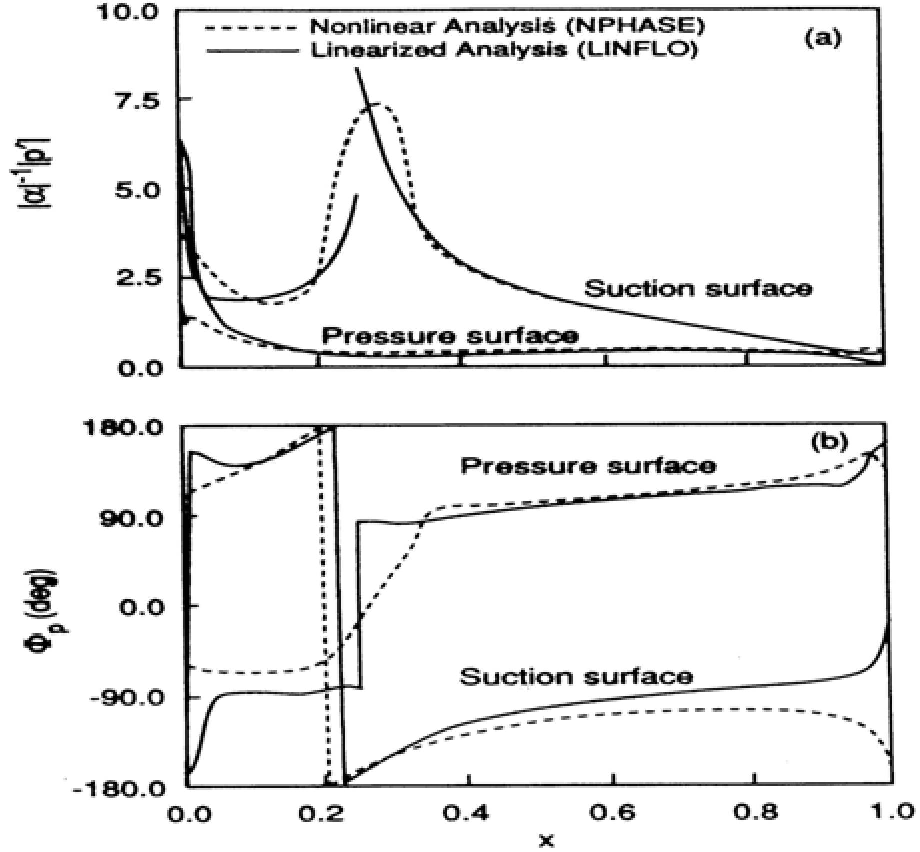

Acoustic Blockage

Magnitude (a) and Phase (b) of the first Harmonic Unsteady Pressure Difference Distribution for the Supersonic Cascade Undergoing an In-Phase Torsional Oscillation of Amplitude a=2º at k1=0.5 about Midchord; M=0.8.

Summary

- RDT unsteady analysis yields good results for subsonic flows.
- RDT unsteady analysis is adequate for transonic flows with local Mach number not exceeding 1.3.
- Strong nonlinear effects resulting from shock boundary layer interaction are significant as the local Mach number exceeds 1.3-1.4.

Aircraft Noise

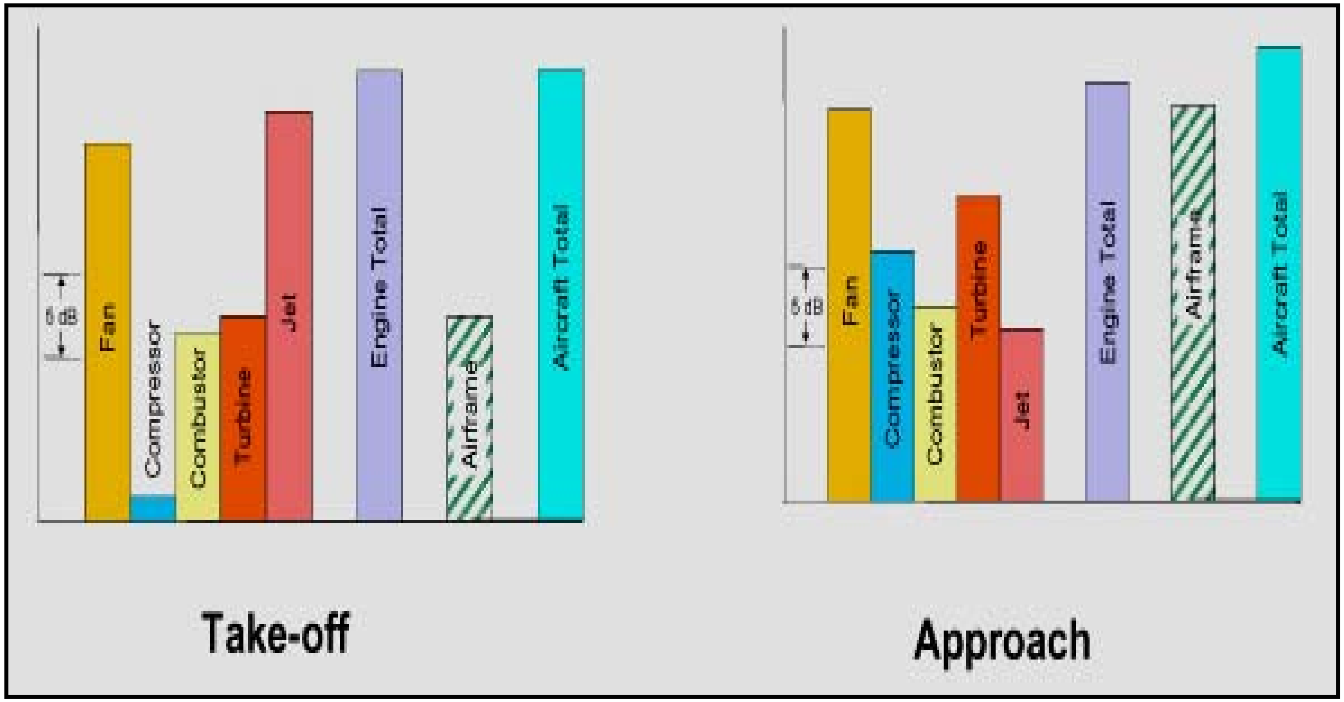

- Fan noise sources:

(high frequency phenomena)

  - Rotor/stator interaction
  - Boundary layers and ingested turbulence
  - Rotor noise

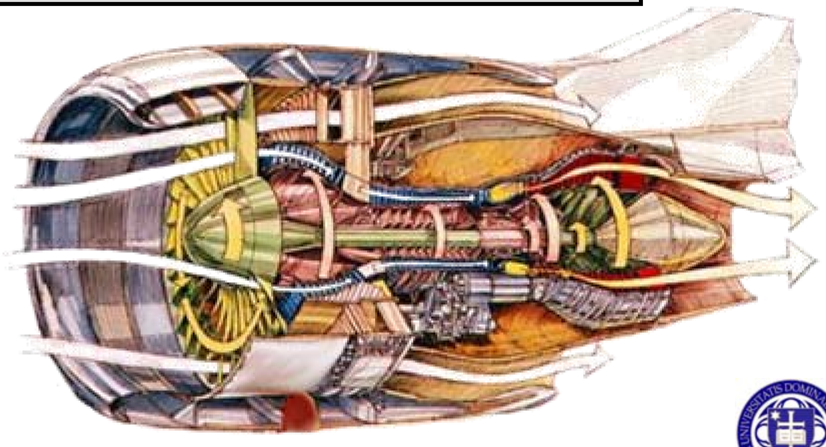

Typical Fan Sound Power Spectra

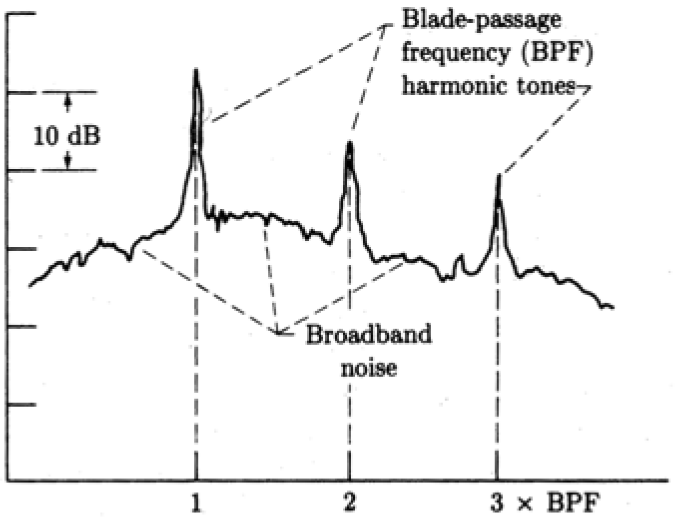

Subsonic Tip Speed

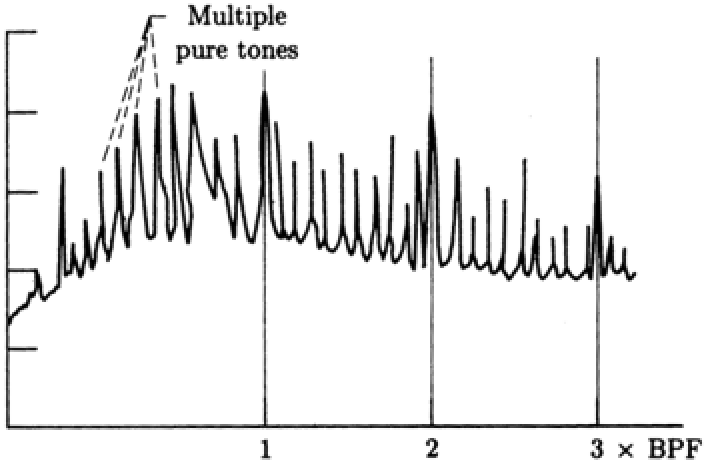

Supersonic Tip Speed

Anatomy of a Turbo-fan Engine

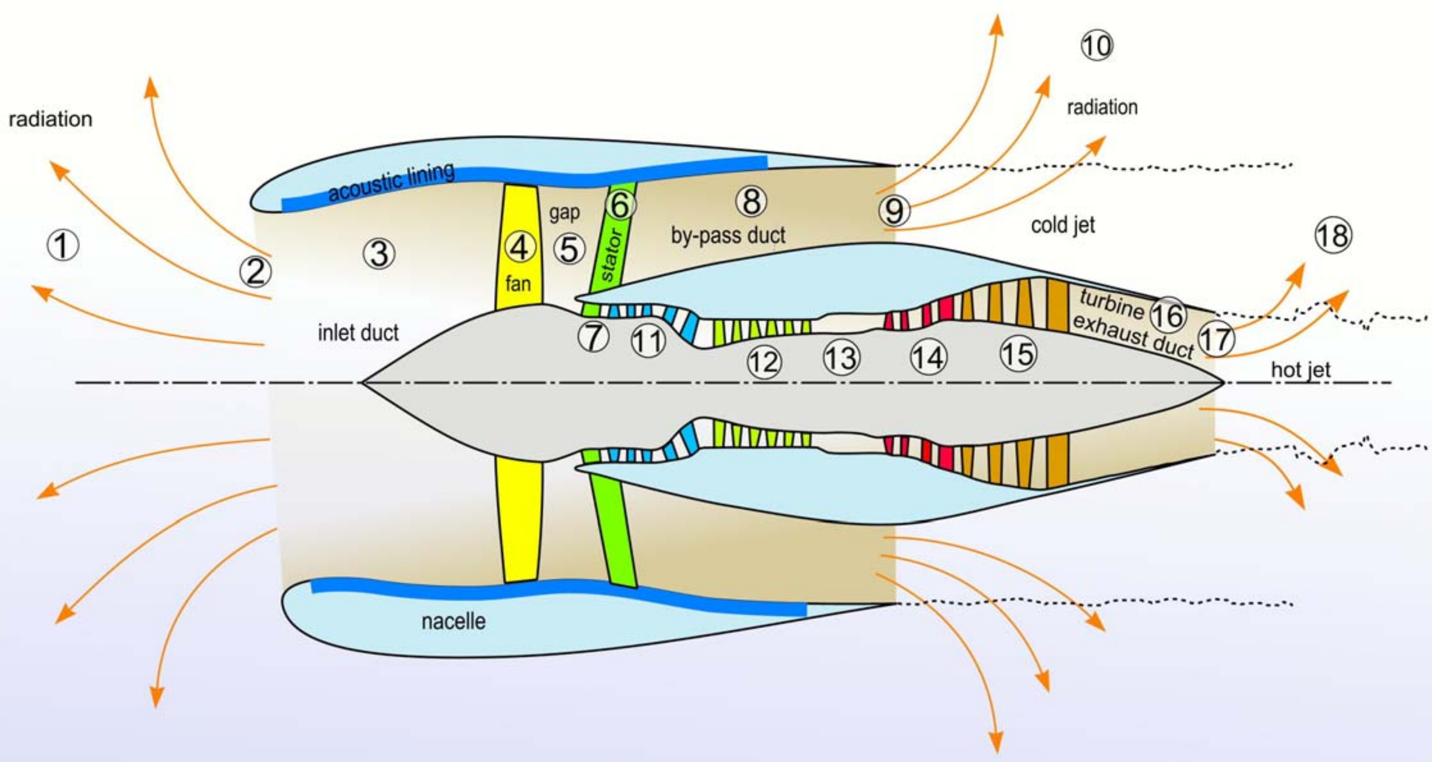

1 = far-field inlet	6 = outlet guide vanes	11 = low-pressure compressor	16 = turbine exhaust duct
2 = inlet plane	7 = engine section stator	12 = high-pressure compressor	17 = hot jet nozzle
3 = inlet duct	8 = bypass duct	13 = combustion chamber	18 = far-field hot exit
4 = fan rotor	9 = cold jet nozzle	14 = high-pressure turbine	
5 = rotor-stator gap	10 = far-field cold exit	15 = low-pressure turbine	

Swirling Flow Phenomena

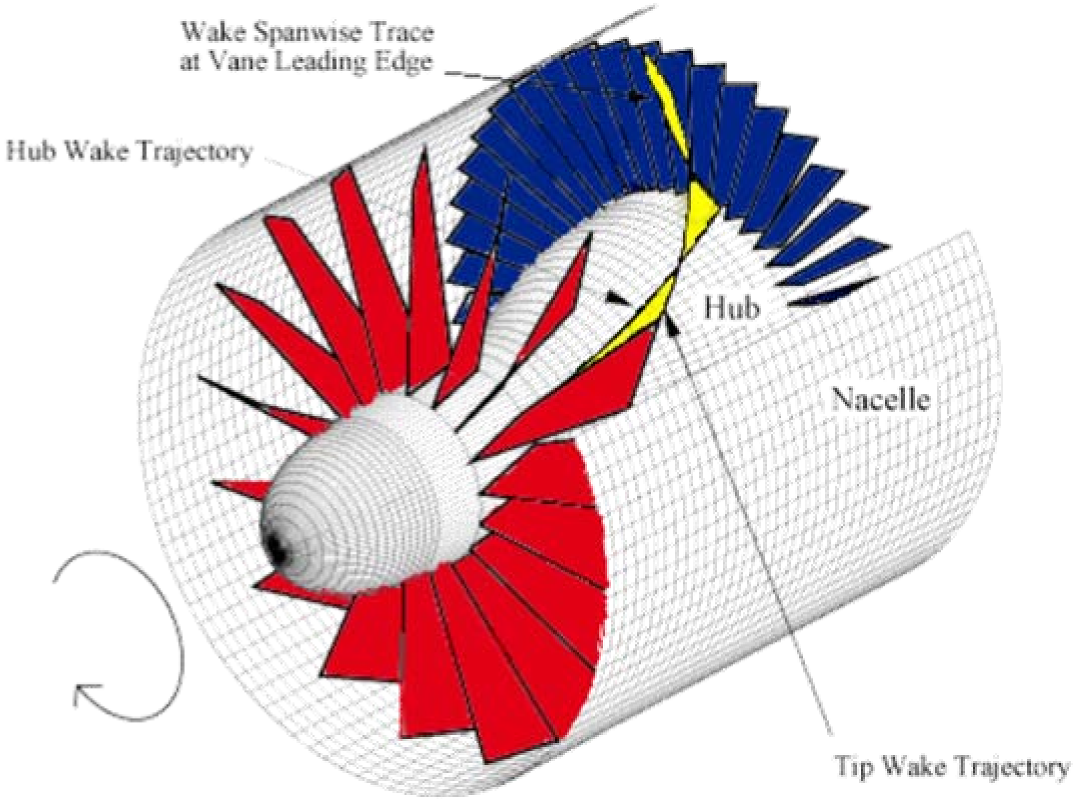

Schematic of Rotor Wake Phenomena

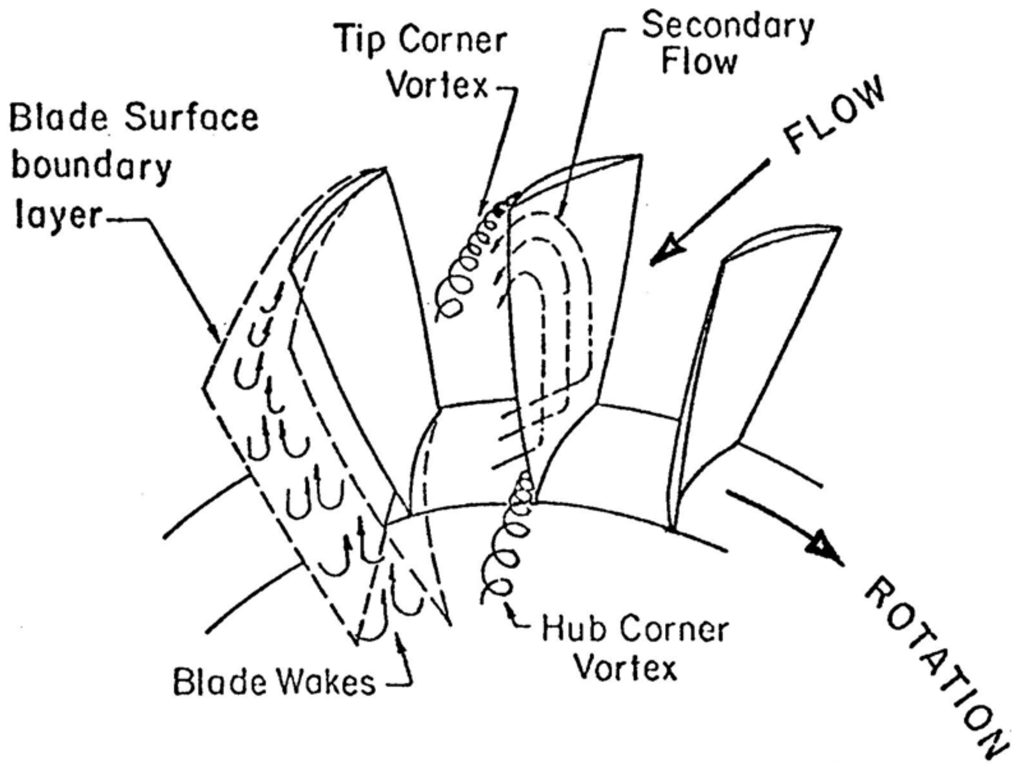

Wake Distortion by Swirl

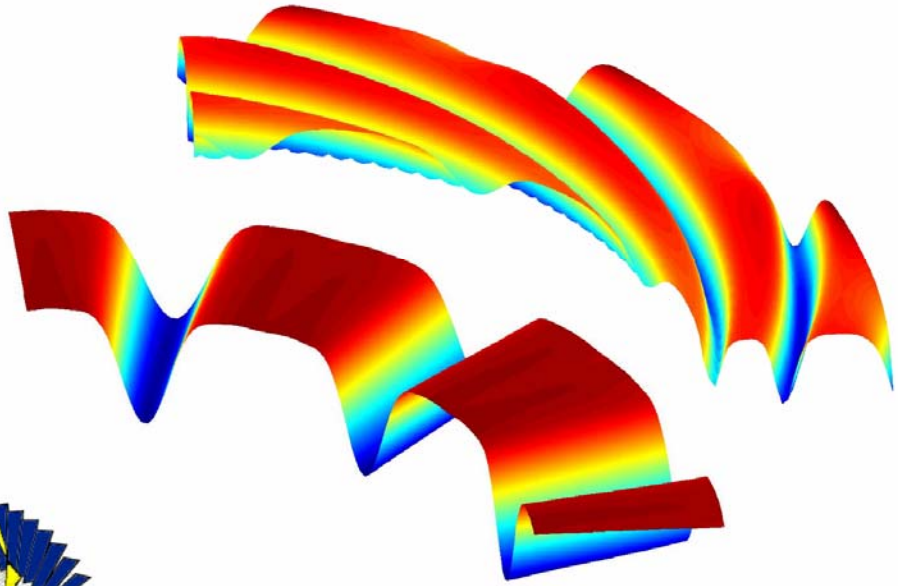

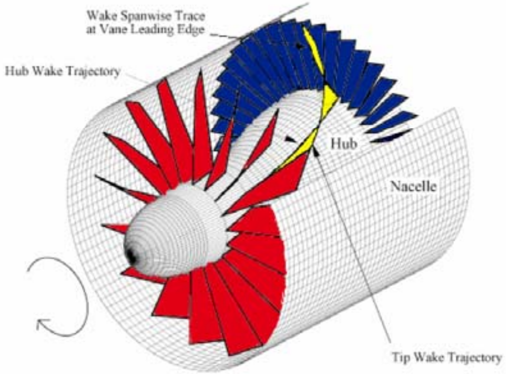

Scaling Analysis

- Two Length Scales:
  - Body Length Scale: ℓ
  - Turbulence Integral Scale = $\Lambda << \ell$
- Two Velocities:
  - Convection velocity: U
  - Speed of sound: c_0
- Aerodynamic Frequencies:

$$\overset{*}{\omega} = \frac{\omega\,\ell}{U} >> 1$$

$$\overset{*}{\omega}' = \frac{\omega\,\Lambda}{U} = O(1)$$

- Acoustic Frequencies

$$\tilde{\omega} = \frac{\omega\,\ell}{c_0}$$

- Fast and Slow Variables:

$$\vec{x}^{\,*} = \frac{\vec{x}}{\ell}$$

$$\tilde{\vec{x}} = \frac{\vec{x}}{\Lambda}$$

Can high frequency help?

Can we turn the scourge to advantage?

Linearized Euler Equations

$$\mathbf{V}(\mathbf{x},t) = \mathbf{U}(x) + \mathbf{u}(x,t)$$

Continuity:

$$\frac{\mathrm{D}}{\mathrm{D}_0\mathrm{t}}\left(\frac{\rho'}{\rho_0}\right) + \frac{1}{\rho_0}\nabla\cdot(\rho_0\mathbf{u}) = 0$$

Momentum:

$$\frac{\mathrm{D}\mathbf{u}}{D_0 t} + \mathbf{u}\cdot\nabla\mathbf{U} = -\nabla\left(\frac{p'}{\rho_0}\right) + \frac{p'}{\rho_0}\frac{\nabla s_0}{c_p} - \frac{s'}{c_p}\frac{\nabla p_0}{\rho_0}$$

Energy:

$$\frac{\mathrm{D}s'}{D_0 t} + \mathbf{u}\cdot\nabla s_0 = 0$$

Thermodynamics:

$$s' = c_v\frac{p'}{p_0} - c_p\frac{\rho'}{\rho_0}$$

Governing Equations in Splitting Form

$$\mathbf{u}(\mathbf{x},t)=\mathbf{u}^{(R)}+\nabla\phi+\frac{s'}{2c_p}\mathbf{U}$$

$$\frac{D_o\mathbf{u}^{(R)}}{Dt}+\mathbf{u}^{(R)}\cdot\nabla\mathbf{U}-\frac{\mathbf{U}}{2c_p}(\mathbf{u}^{(R)}.\nabla s_0)=\nabla\phi\times(\nabla\times\mathbf{U})-\frac{D_o\phi}{Dt}\frac{\nabla s_0}{c_p}+\frac{\mathbf{U}}{2c_p}(\nabla\phi\cdot\nabla s_0)$$

$$\frac{D_o}{Dt}\left(\frac{1}{c_0^2}\frac{D_o\phi}{Dt}\right)-\frac{1}{\rho_0}\nabla(\rho_0\nabla\phi)-\frac{\nabla\phi.\nabla s_0}{c_p}=\frac{1}{\rho_0}\nabla(\rho_0\mathbf{u}^{(R)})+\frac{\mathbf{u}^{(R)}.\nabla s_0}{c_p}+\frac{\mathbf{U}\cdot\nabla s'}{2c_p}$$

$$\frac{D_o s'}{Dt}+\mathbf{u}\cdot\nabla s_o=0$$

$$s'-c_v\frac{p'}{p_0}+c_p\frac{\rho'}{\rho_0}=0$$

$$p'=-\rho_0\frac{D_o}{Dt}\phi$$

Normal Mode Analysis

Normal Mode Analysis

- A normal mode analysis of linearized Euler equations is carried out assuming solutions of the form

$$f(r)e^{i(-\omega t + m_\nu \theta + k_{mn} x)}$$

- Eigenvalue problem is not a Sturm-Liouville type and singular for vanishing

$$\Lambda_{mn} = \frac{D_0}{Dt} = -\omega + k_{mn} U_x + \frac{mU_s}{r}$$

- A combination of spectral and shooting methods is used in solving this problem

Mode Spectrum
Spectral and Shooting Methods

P&W mean flow data, ω=16, and m=-1

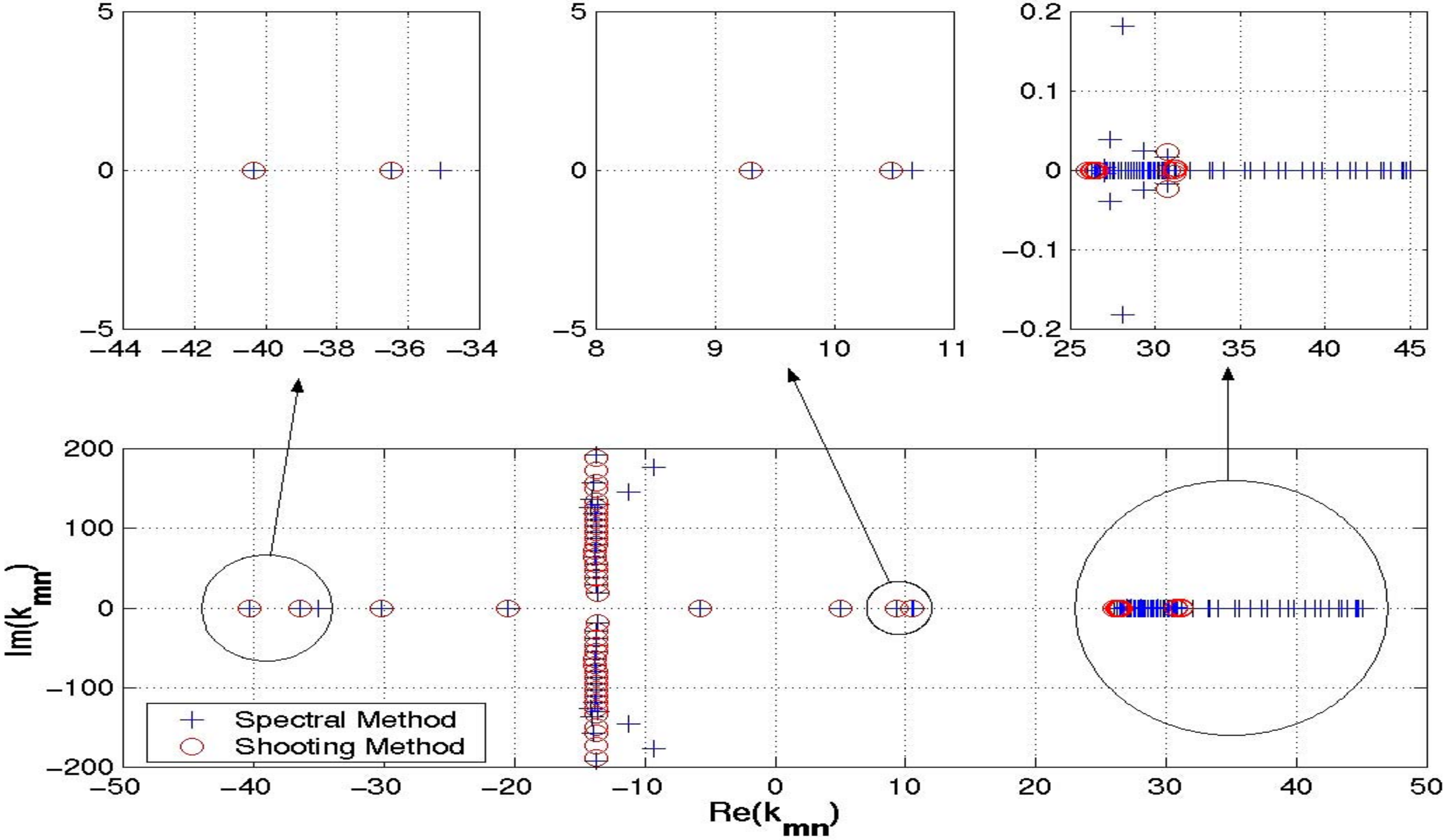

Coupling Between Pressure, Vorticity, and Entropy

Non-isentropic flow M_x=0.3, M_Γ=0.3, M_Ω=0.3, ω=10, and m=2

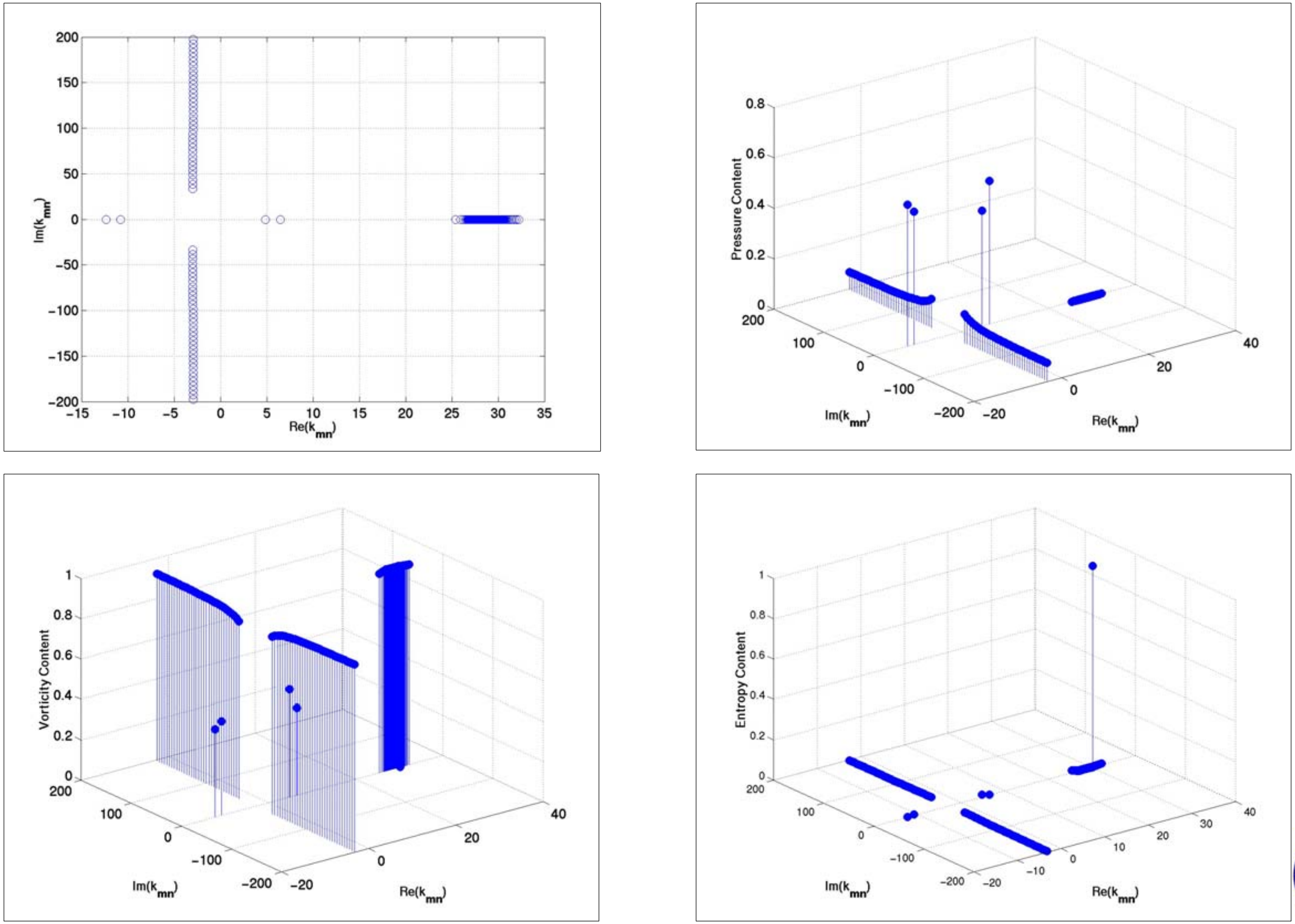

Effect of Swirl on Eigenmode Distribution

$M_{xm=}0.56$, $M_{\Gamma}=0.25$, $M_{\Omega}=0.21$

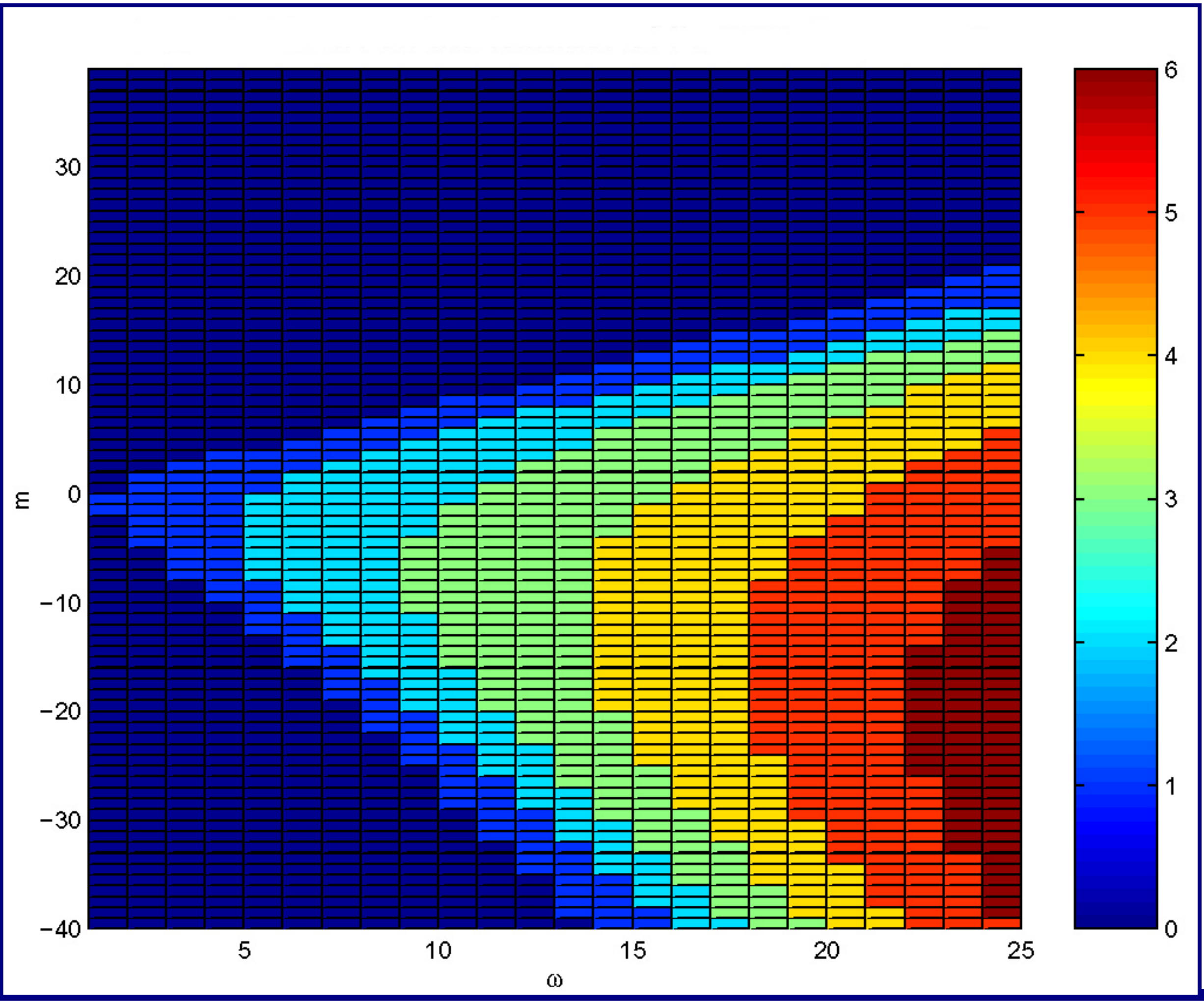

Upstream Representation of Disturbances

Upstream Disturbance Representation (1)

Uniform Flow

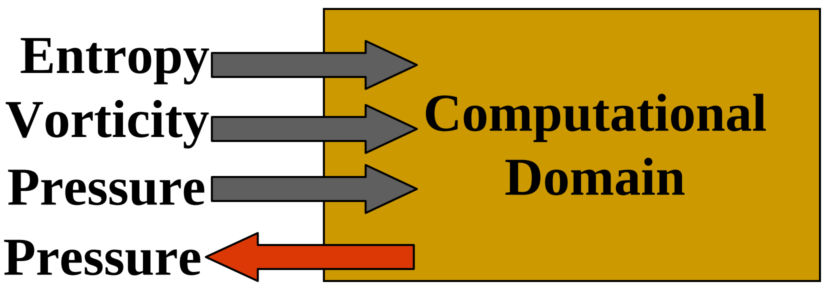

$$\vec{u} = \vec{u}_R + \nabla\Phi$$

Vortical velocity is solenoidal

$$\nabla \bullet \vec{u}_R = 0$$

Nonuniform Flow

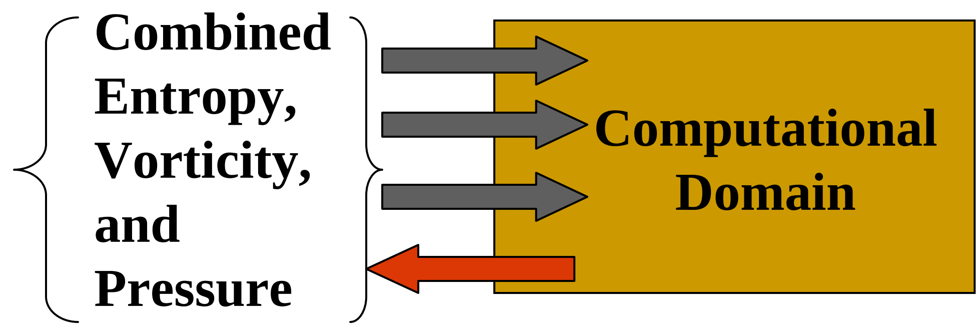

??

Upstream Disturbance Representation (2)

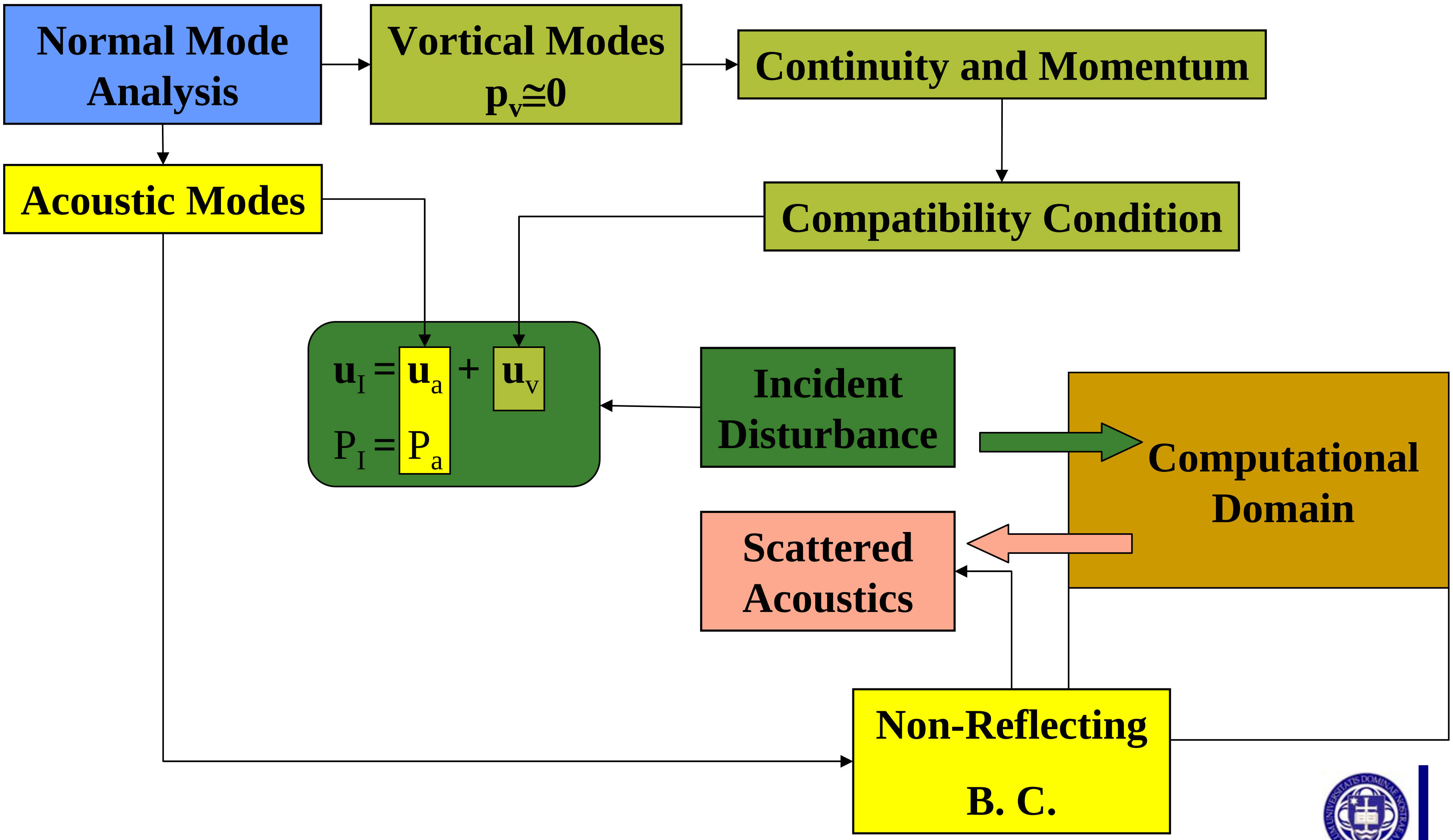

Nonreflecting Boundary Conditions

Nonreflecting Boundary Conditions

- Pressure at the boundaries is expanded in terms of the acoustic eigenmodes.

$$p(\vec{x},t) = \int_{\omega} \sum_{\nu=-\infty}^{\infty} \sum_{n=0}^{\infty} c_{mn}\, p_{mn}(\omega, r) e^{i(-\omega\ t + m_{\nu}\theta + k_{mn} x)} d\omega$$

- Only outgoing modes are used in the expansion.
- Group velocity is used to determine outgoing modes.

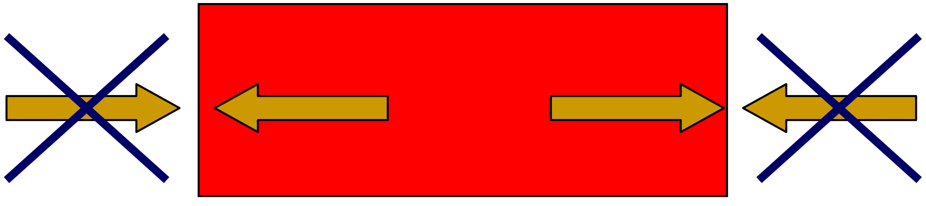

Causality

Nonreflecting Boundary Conditions (Cont.)

$$p(\vec{x},t) = \sum_{\nu=-M/2}^{M/2} \sum_{n=0}^{N} c_{mn}\, p_{mn}(r) e^{i(-\omega t + m_\nu \theta + k_{mn} x)}$$

$$[p] = [\Re][c]$$

$$[p]_{L-1} = [\Re]_{L-1}[c]$$

$$[p]_{L} = [\Re]_{L}[c]$$

$$[p]_{L} = [\Re]_{L}[\Re]_{L-1}^{-1}[p]_{L-1}$$

Aerodynamic-Aeroacoustic Model

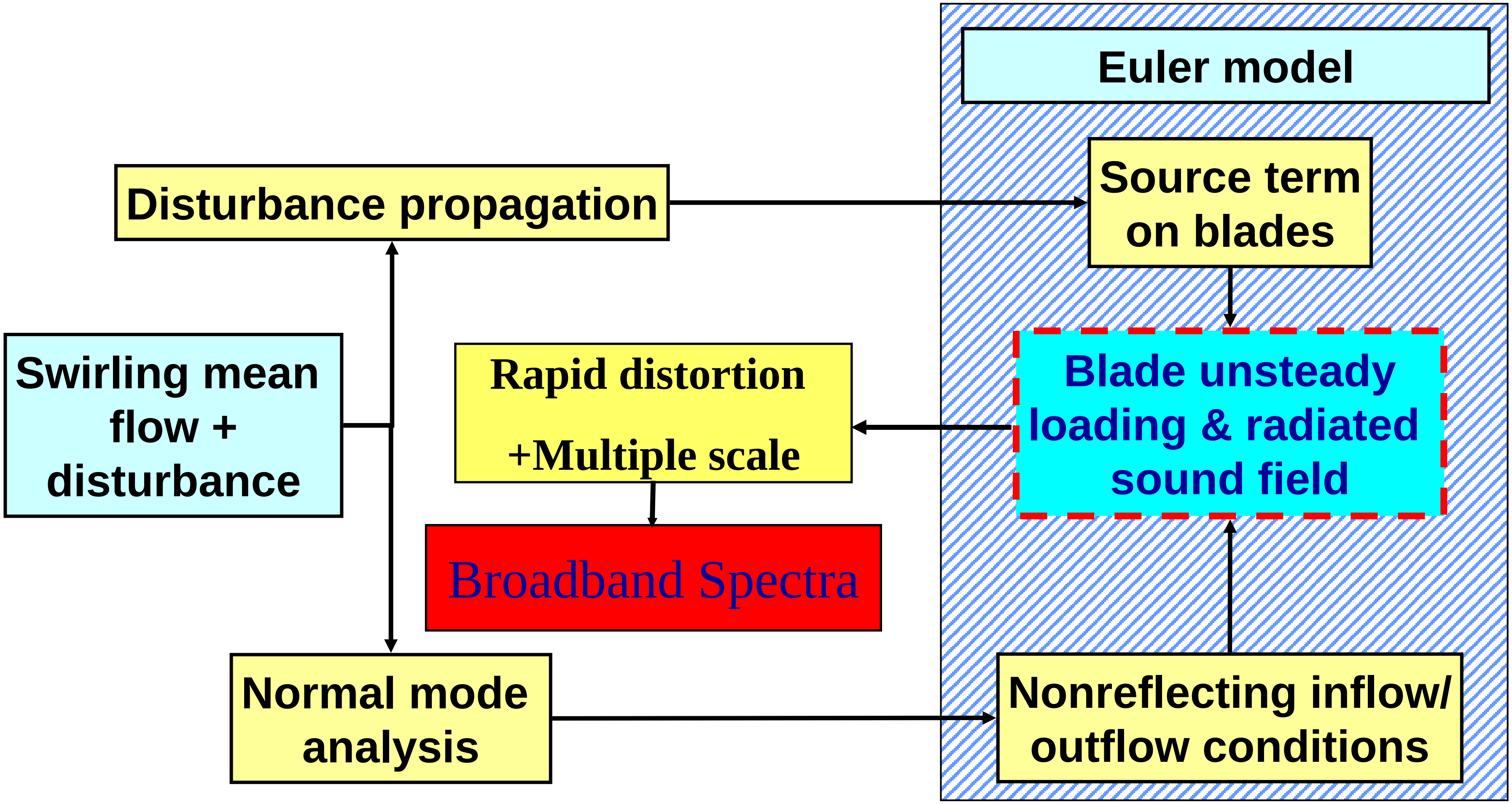

Schematics of the Computational Domain

High frequency asymptotics come to help

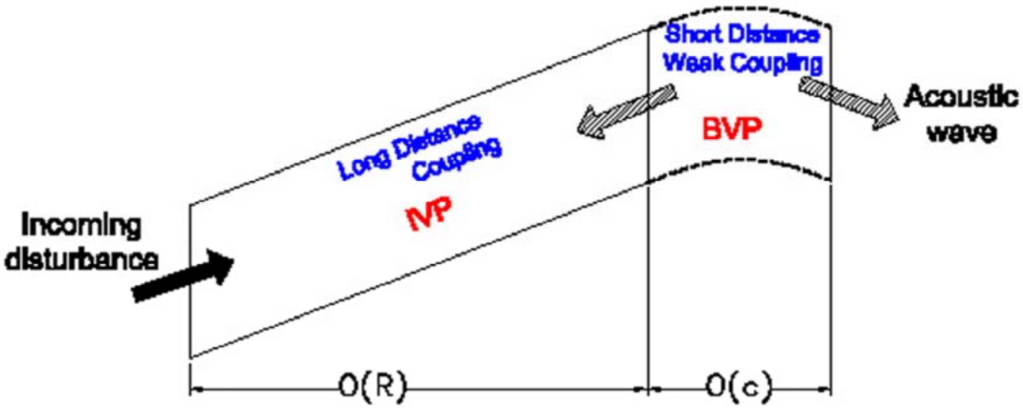

Domain Decomposition of
the Computational Domain

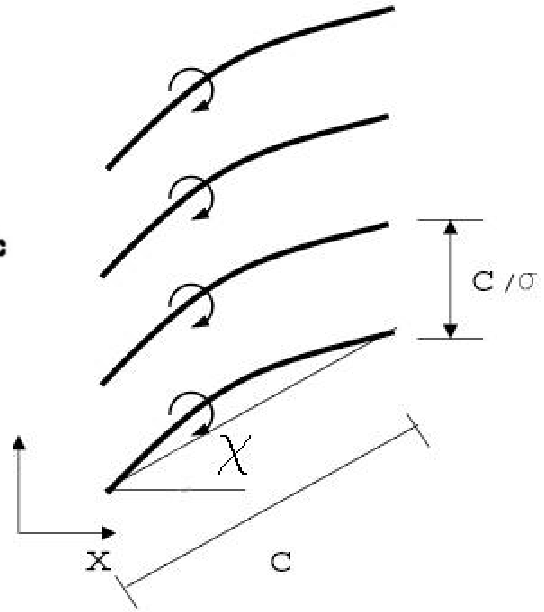

The Annular Cascade

Incidence Disturbance Coupling with duct Modes B=16, V=24, c=2π/24, r_h/r_t=0.5, L=3c

- Often the largest amplitudes of the incident vortical disturbances occur in either the hub and tip regions of the duct where viscous effects result in significant intensification of the wake.

- Hub-dominated incident disturbance:

$$a_{m_g}^{(u)} = \cos \frac{\pi}{2} \frac{r - r_h}{r_t - r_h}$$

- Tip-dominated incident disturbance:

$$a_{m_g}^{(u)} = \cos \frac{\pi}{2} \frac{r_t - r}{r_t - r_h}$$

Profile of the First Downstream and Upstream Modes

-Uniform Flow, -- Rigid body swirl, -.- Free vortex swirl
$\omega = 2.5\,\pi$

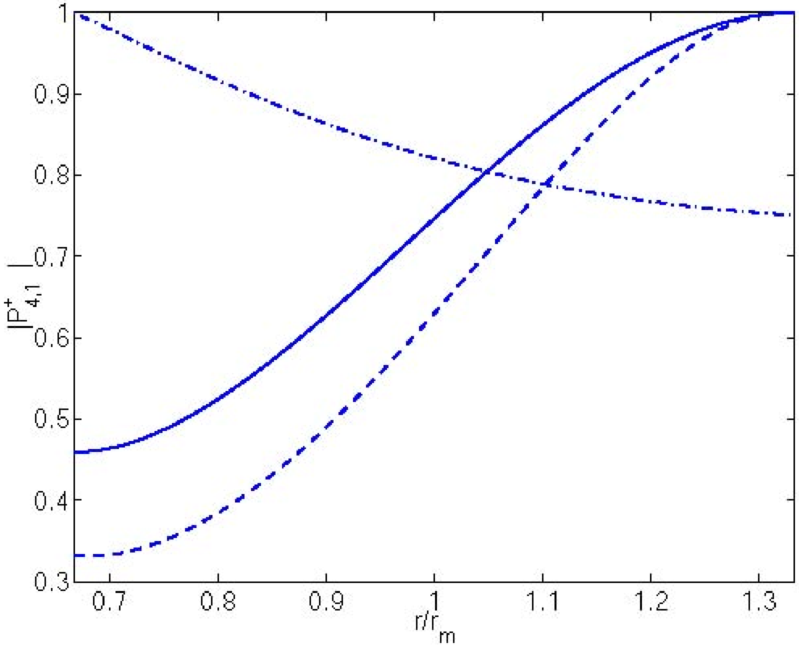

Downstream

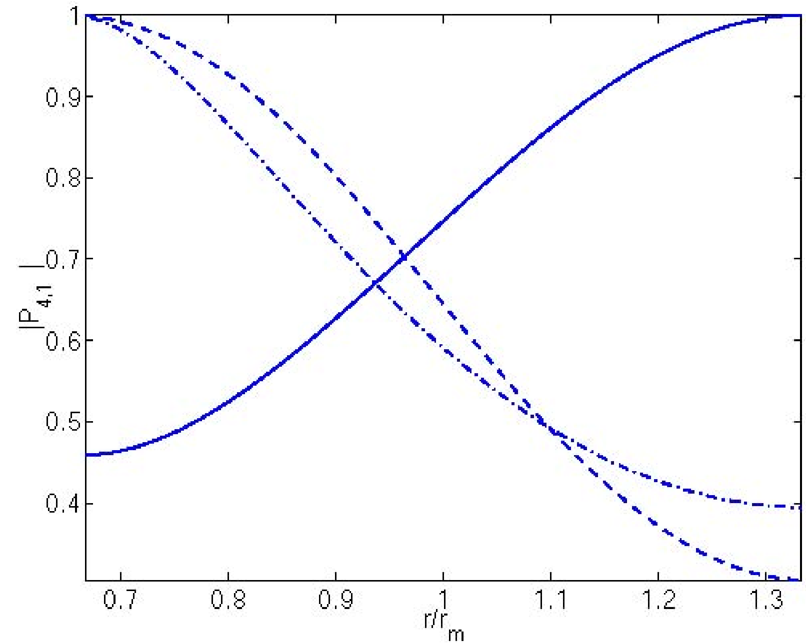

Upstream

Magnitude of the upstream and downstream acoustic modes $\omega=2.5\pi$

	n	CASE1 hub-dominated $\lvert c^+_{mn}\rvert$	CASE1 hub-dominated $\lvert c^-_{mn}\rvert$	CASE 2 tip-dominated $\lvert c^+_{mn}\rvert$	CASE 2 tip-dominated $\lvert c^-_{mn}\rvert$
Uniform Flow $M_x=0.4$ $M_\Omega=0.0$ $M_\Gamma=0.0$	1	0.048 (ht)	0.040 (ht)	0.059 (tt)	0.053 (tt)
	2	0.099 (hh)	0.073 (hh)	0.009 (th)	0.008 (th)
Rigid Body Swirl $M_x=0.4$ $M_\Omega=0.0$ $M_\Gamma=0.0$	1	0.083 (ht)	0.018 (hh)	0.102 (tt)	0.030 (th)
	2	0.110 (hh)	0.025 (hh)	0.020 (th)	0.049 (th)
Potential Swirl $M_x=0.4$ $M_\Omega=0.0$ $M_\Gamma=0.0$	1	0.018 (hh)	0.009 (hh)	0.038 (th)	0.016 (th)
	2	0.017 (hh)	0.006 (hh)	0.075 (th)	0.028 (th)

Comparison of Acoustic Response of 2D and 3D Cascades to a Harmonic Excitations

- ω=30.50
- m_g=16
- n_g=0
- h_r/h_t = 0.6
- M=0.5
- Stagger= 0^o and 30^o
- Swirl $M_\Gamma = M_\Omega$ =0.125 (at r_m)
- Blade Number=24
- Spacing=1

Acoustic Response and Axial Wave Number of a 2D Linear Cascade

ω=30.50, m_g=16, n_g=0, M=0.5, stagger=30°, B=24, s/c =1

Downstream

m	n	k_{mn}	$\|c_{mn}\|$
16	0	7.6081	**0.0542**
-8	0	17.6352	**0.0375**
-32	0	2.1685	**0.0708**

Upstream

m	n	K_{mn}	$\|c_{mn}\|$
16	0	29.9700	**0.0189**
-8	0	46.4075	**0.0371**
-32	0	37.2995	**0.0177**

3 propagating modes ($n=n_g$)

Top View of the Acoustic Pressure of a 2D Linear Cascade

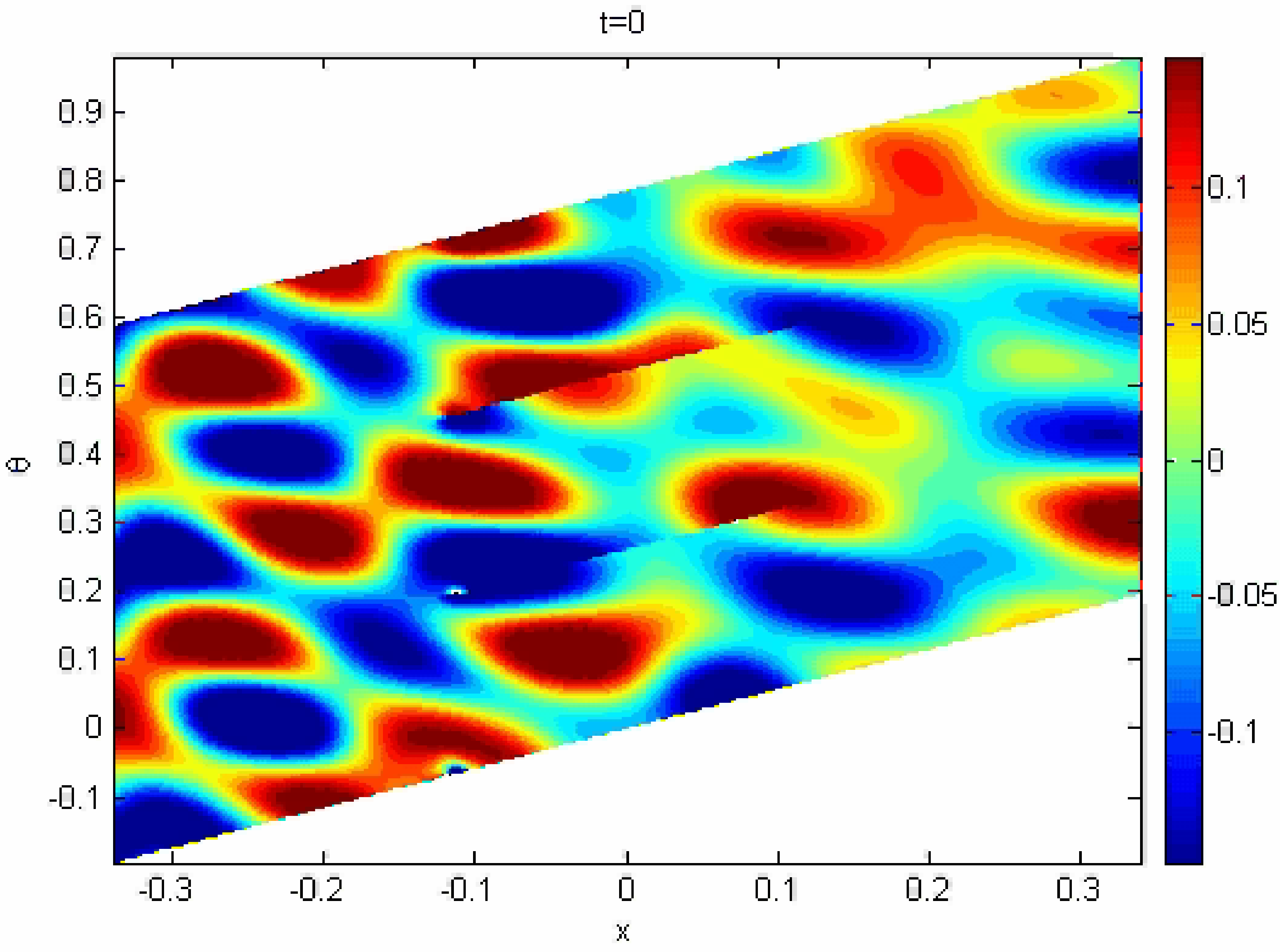

Acoustic Response and Axial Wave Number of a 3D Annular Cascade

ω=30.50, m_g=16, n_g=0, M=0.5, stagger=0°, B=24, s/c =1, $h_r/h_t = 0.6$

Downstream

m	n	k_{mn}	| $\|c_{mn}\|$
16	0	12.1905	**0.1090**
16	1	8.9474	**0.0595**
16	2	5.7227	0.0374
16	3	-0.5668	0.0196
-8	0	15.4739	0.0449
-8	1	14.2355	0.0216
-8	2	11.7102	0.0189
-8	3	6.6571	0.0079
-8	4	-3.3952	0.0041
-32	0	-7.1684	**0.1449**

Upstream

m	n	k_{mn}	$\|c_{mn}\|$
16	0	-32.7664	0.0293
16	1	-39.0561	0.0202
16	2	-42.2807	**0.0696**
16	3	-45.5238	**0.0414**
-8	0	-29.9381	0.0032
-8	1	-39.9905	0.0074
-8	2	-45.0435	0.0134
-8	3	-47.5688	0.0114
-8	4	-48.8073	0.0125
-32	0	-26.1648	**0.1560**

10 propagating modes

Top View of the Acoustic Pressure of a 3D Annular Cascade
Zero- Stagger

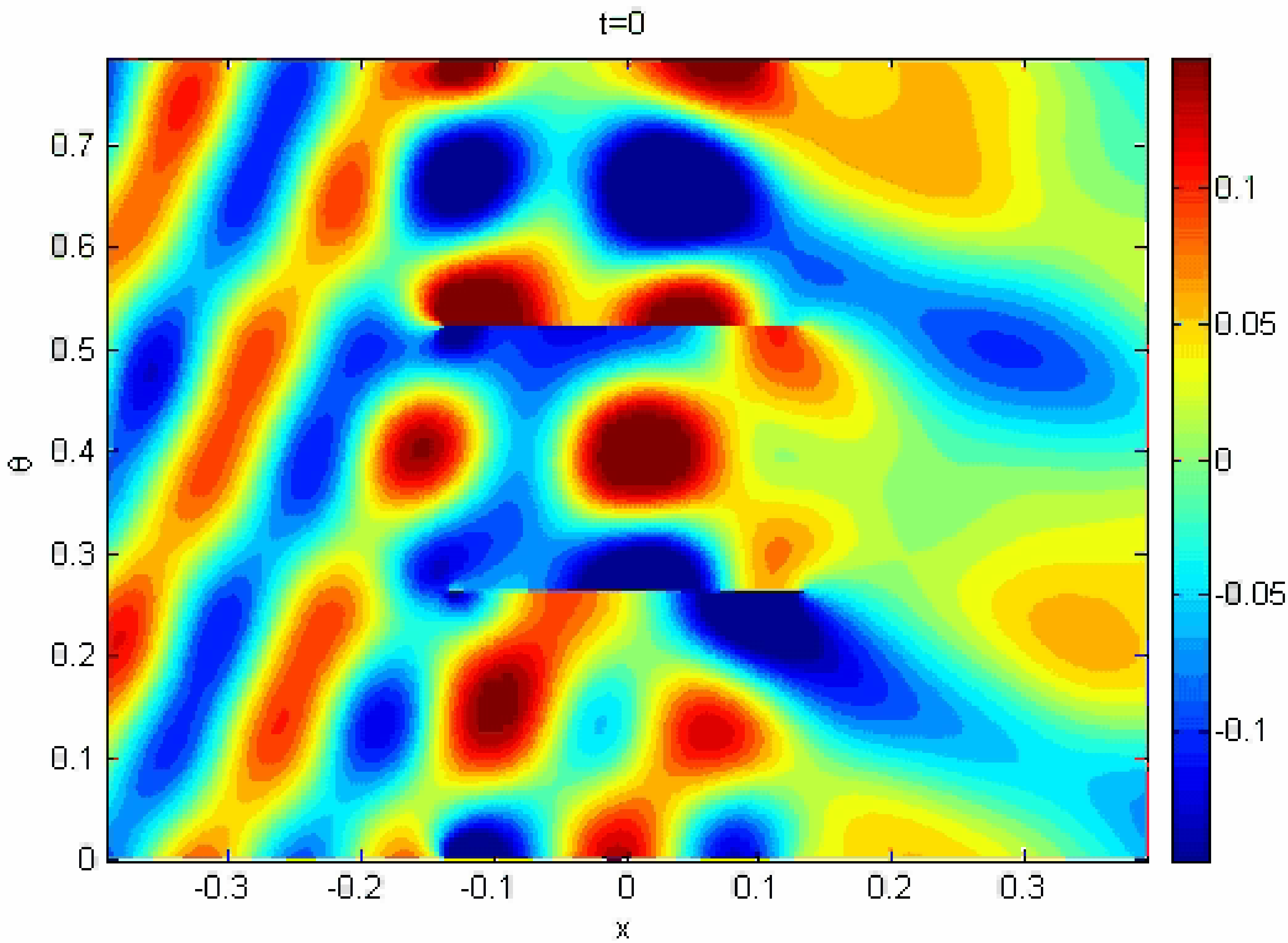

Acoustic Response and Axial Wave Number of a 3D Annular Cascade

ω=30.50, m_g=16, n_g=0, M=0.5, stagger=30°, B=24, s/c =1, $h_r/h_t = 0.6$

Downstream

m	n	k_{mn}	$\lvert c_{mn} \rvert$
16	0	9.8459	0.0519
16	1	4.4321	**0.0736**
16	2	-2.1739	**0.1162**
-8	0	17.8059	0.0659
-8	1	16.6875	0.0356
-8	2	14.3758	0.0115
-8	3	9.8157	0.0098
-8	4	1.3140	0.0028
-32	0	7.5623	**0.0882**
-32	1	-0.2123	0.0382
-32	2	-10.8543	0.0436

Upstream

M	n	k_{mn}	$\lvert c_{mn} \rvert$
16	0	-20.4406	**0.1097**
16	1	-26.6919	**0.0794**
16	2	-30.8843	**0.0811**
-8	0	-30.1154	0.0043
-8	1	-38.5356	0.0125
-8	2	-42.7368	0.0093
-8	3	-44.9057	0.0281
-8	4	-48.4882	0.0235
-32	0	-25.7269	0.0267
-32	1	-33.9841	0.0241
-32	2	-38.6116	0.0148

11 propagating modes

Top View of the Acoustic Pressure of a 3D Annular Cascade
30^o- Stagger

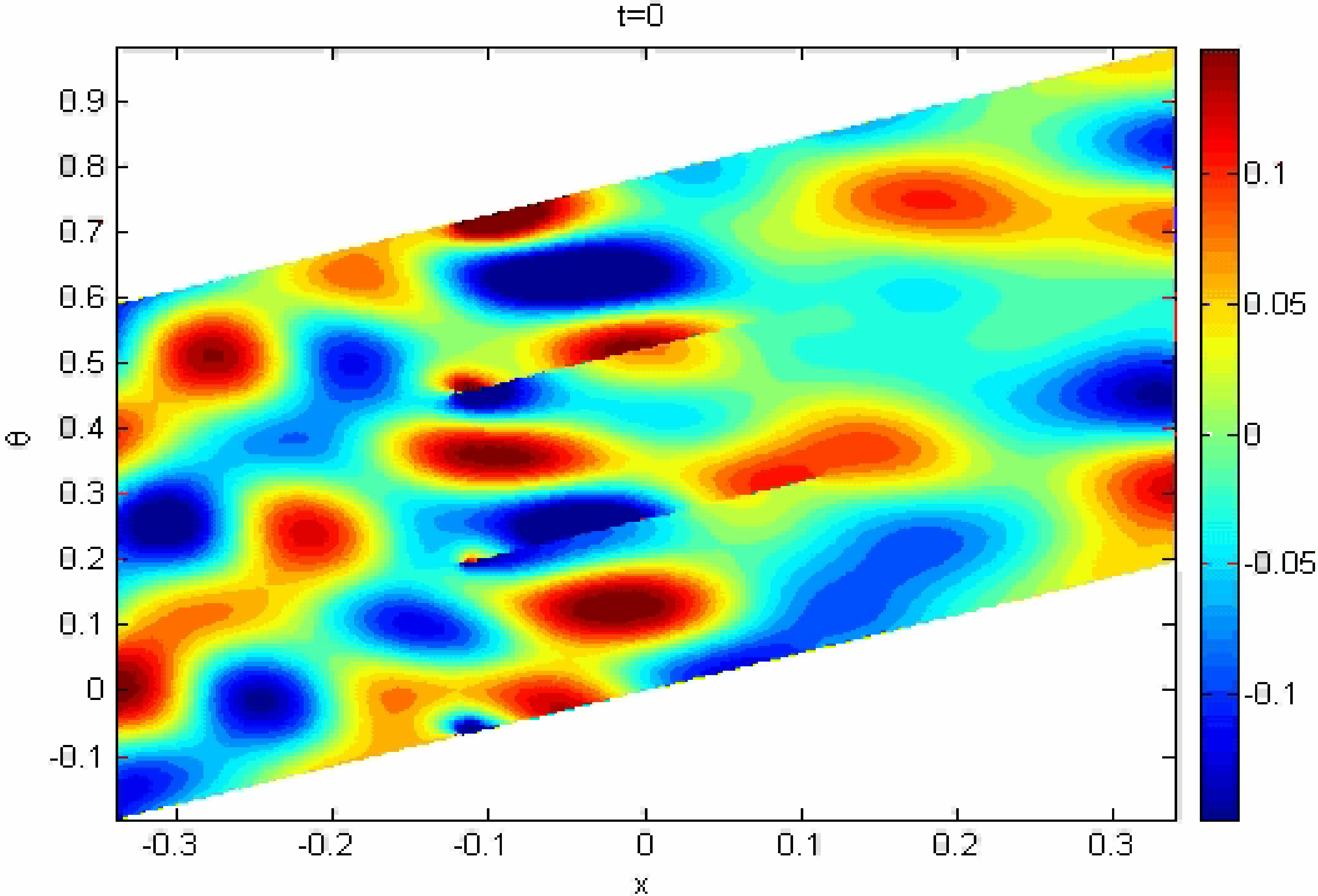

Summary for Tonal Noise Response of an Annular Cascade

- The nonuniform swirling flow changes the physics of scattering in 3 major ways:
  - It increase the number of acoustic modes in the duct.
  - It changes their duct radial profile.
  - It causes significant amplitude and radial phase variation of the incident disturbances.
- The higher number of cut-on modes is due to the fact that the acoustic radial mode number, n, is no longer restricted to be equal to that of the upstream excitation, i.e., $n=n_g$.
- When the radial phase of the incident disturbance is different from that of the duct modes, weak scattering occurs.
- Analysis of the radial variation of the incident disturbance and duct modes can provide an indication of the efficiency of the scattering process.
- Results suggest that 2D models underestimate the acoustic power by 3db at moderately high frequencies.

Hanson's Cascade
Scattered Acoustic Power versus Frequency

- $h_r/h_t = 0.6$
- $M=0.5$
- Stagger= 0^o and 30^o (at r_m)
- Swirl : $M_\Gamma = M_\Omega = .125$ (at r_m)
- Blade Number=45
- Spacing = 0.8
- Turbulence Integral Scale = $0.032\ r_{(0.85)}$
- Turbulence Level/Mean Velocity = 0.018

Acoustic Power Level versus Frequency for an Annular Cascade at 35° Stagger Comparison with 2D Strip Theory

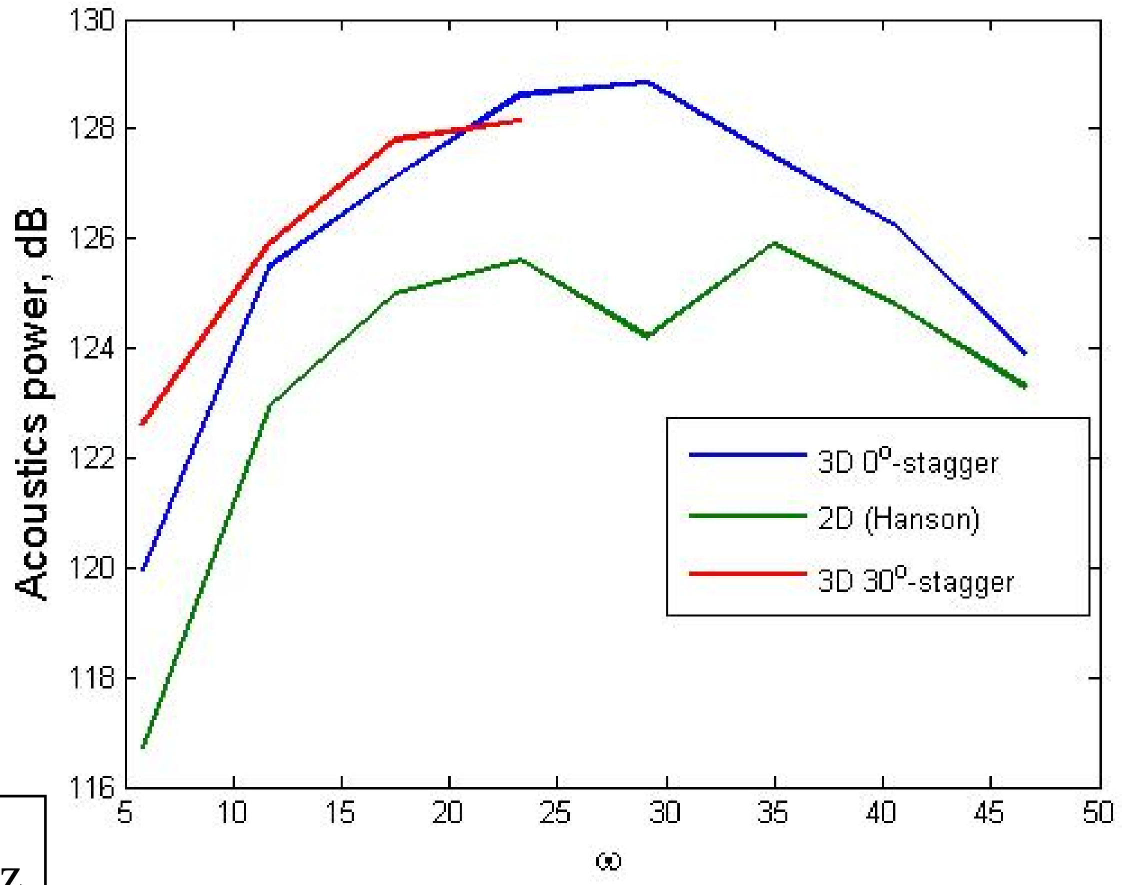

ω=35, 1000 Hz

High Frequency Case

High frequency asymptotics come again to help

- At high frequency, the inflow disturbance interaction with the cascade is dominated by local effects. Airfoil theory suggests that the acoustic pressure has a simple dependence on the the frequency of the form $1/\omega^{\alpha}$.
- for $\omega > 1/\Lambda$, the turbulence spectral density also has a simple dependence on frequency and dominates the contribution to the scattered broadband energy.

$$c_{mn} \sim \omega^{-\frac{1}{2}}$$

$$\text{For} \quad k >> \frac{1}{\Lambda}$$

Liepmann' spectrum :

$$\Phi_{ij} \sim \frac{1}{\omega^4}, \quad P(\omega) \sim \frac{1}{\omega^3}$$

DATA :

$$\Phi_{ij} \sim \frac{1}{\omega^{11/3}}, \quad P(\omega) \sim \frac{1}{\omega^{2.66}}$$

Reduction of Hanson's Results (stagger 30o)

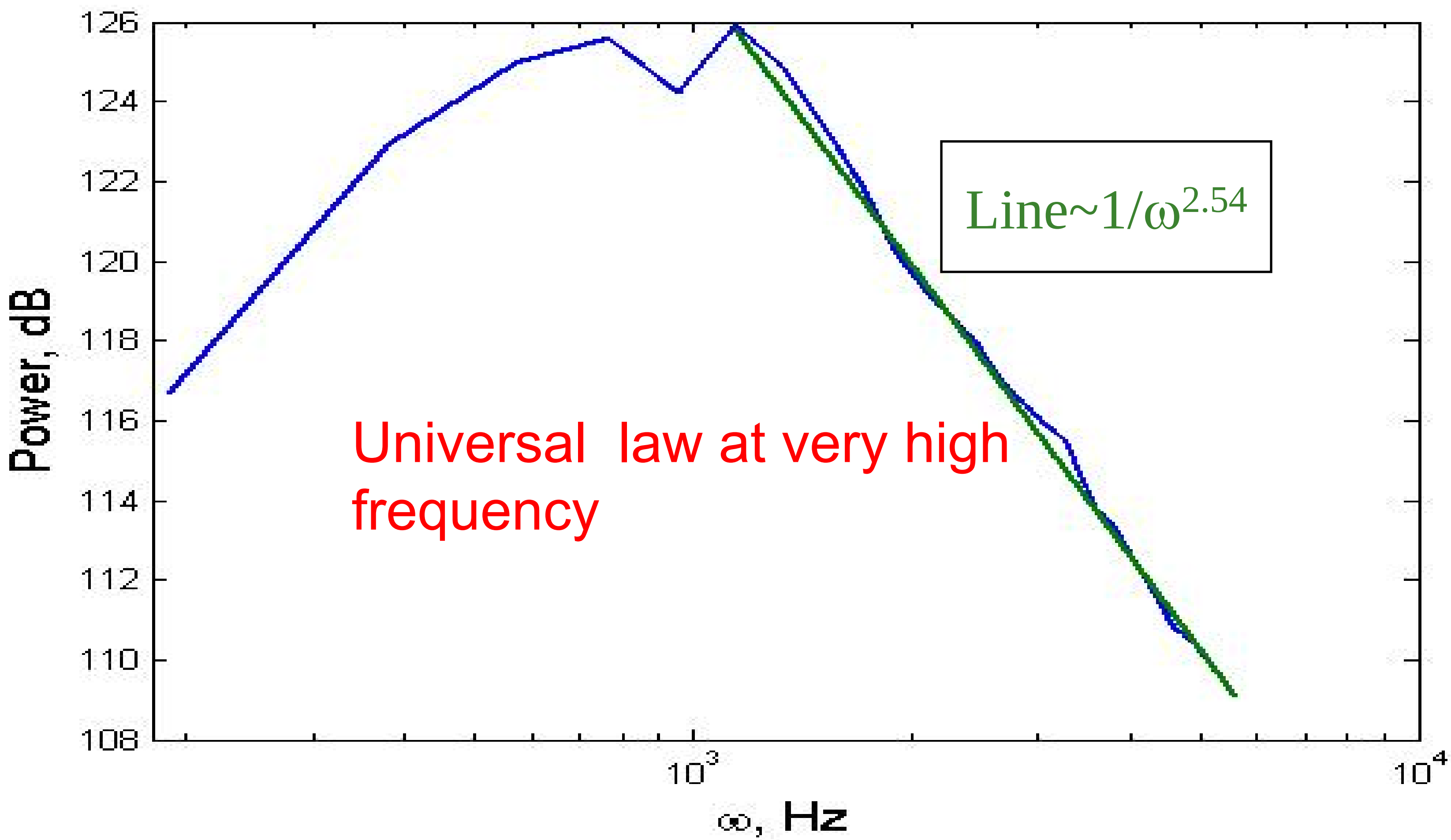

1000Hz, ω= 35.

Conclusions fro Broadband Noise

- At moderate frequencies the 3D model yields higher level of noise.
- At high frequency (ω>>1/ Λ) asymptotic analysis and preliminary results suggest the scattered acoustic power, P~ 1/ ω^{α} with 2.3<α<2.75.
- This obviates the need to calculate the scattered acoustic power for the computationally intensive high frequencies.
- Comparison with experimental results is planned.

Tonal and Broadband Sources of Noise in a Ducted Propeller

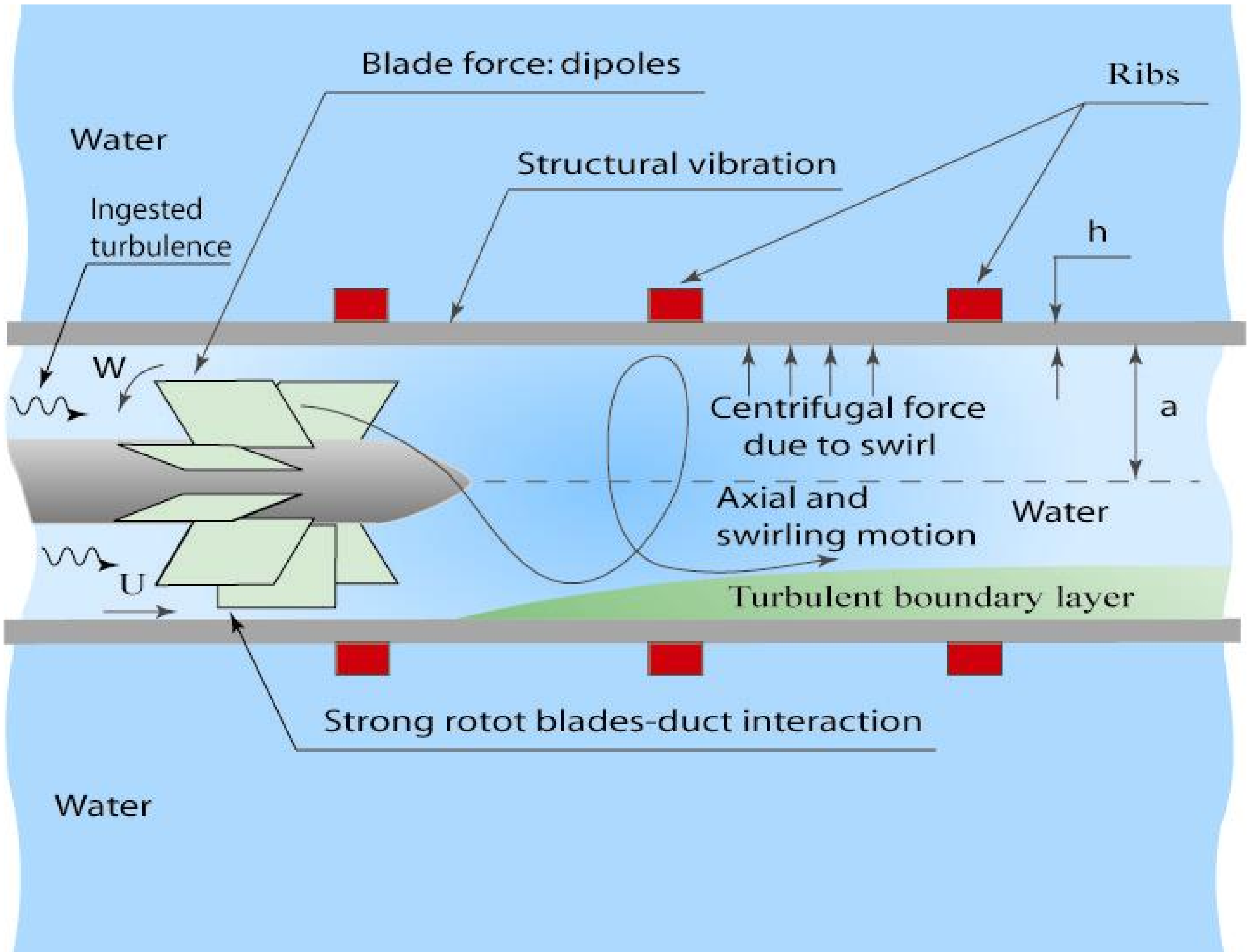

Issues for Consideration

- How does coupling the flow-propeller interaction to the elastic duct system affect the propeller distributed dipole sources?
- Determine Transfer Functions for Acoustic Radiation for Various Duct Conditions.
- What conditions may lead to strong coupling between hydrodynamic disturbances and the elastic duct?

Coupling the propeller with the system

- Duct boundary condition determines duct modes and blade hydrodynamic response(dipole strength and orientation)
  - Rigid duct: $u_r=0$.
  - Elastic duct: duct impedance determines duct modes
    - Dynamical Stiffness: $p'=D(a, h, E, \nu, \alpha, \omega)\, \zeta_r$
    - Impedance: $Z=R+iX = i\, D/\omega$
    - Fluid mode relation: $p'=\Pi(\alpha, \omega, a, \rho)\, u_r$
    - Dispersion equation:

$$\Pi(\alpha, \omega, a, \rho) = Z(a, h, E, \nu, \alpha, \omega)$$

Natural in Vacuo Wave Numbers versus Frequency for Different Circumferential Mode Numbers m=0,1,2,3.

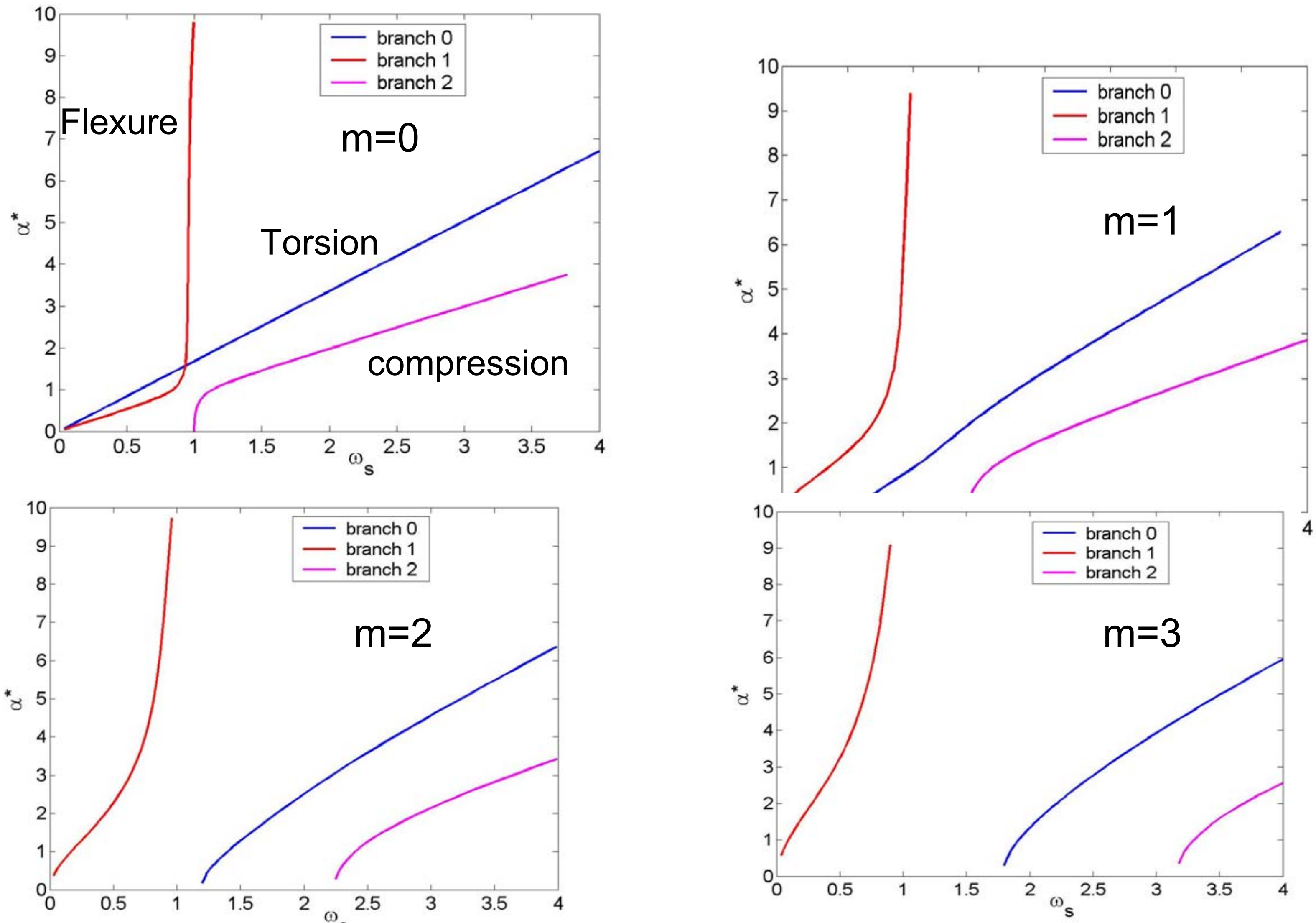

Copper/Water Dispersion Relation
Submerged Duct

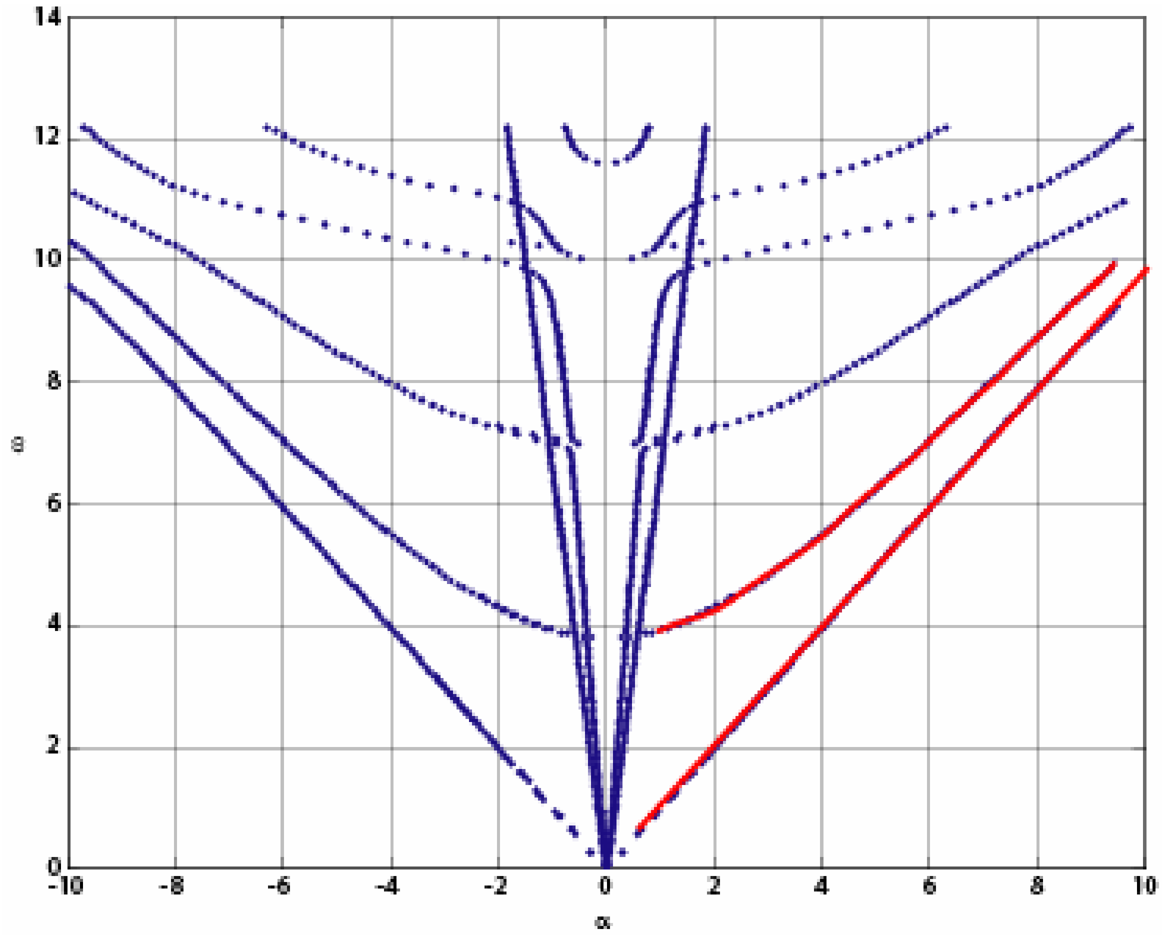

Copper/Water Dispersion Relation

Submerged Duct with Ribs

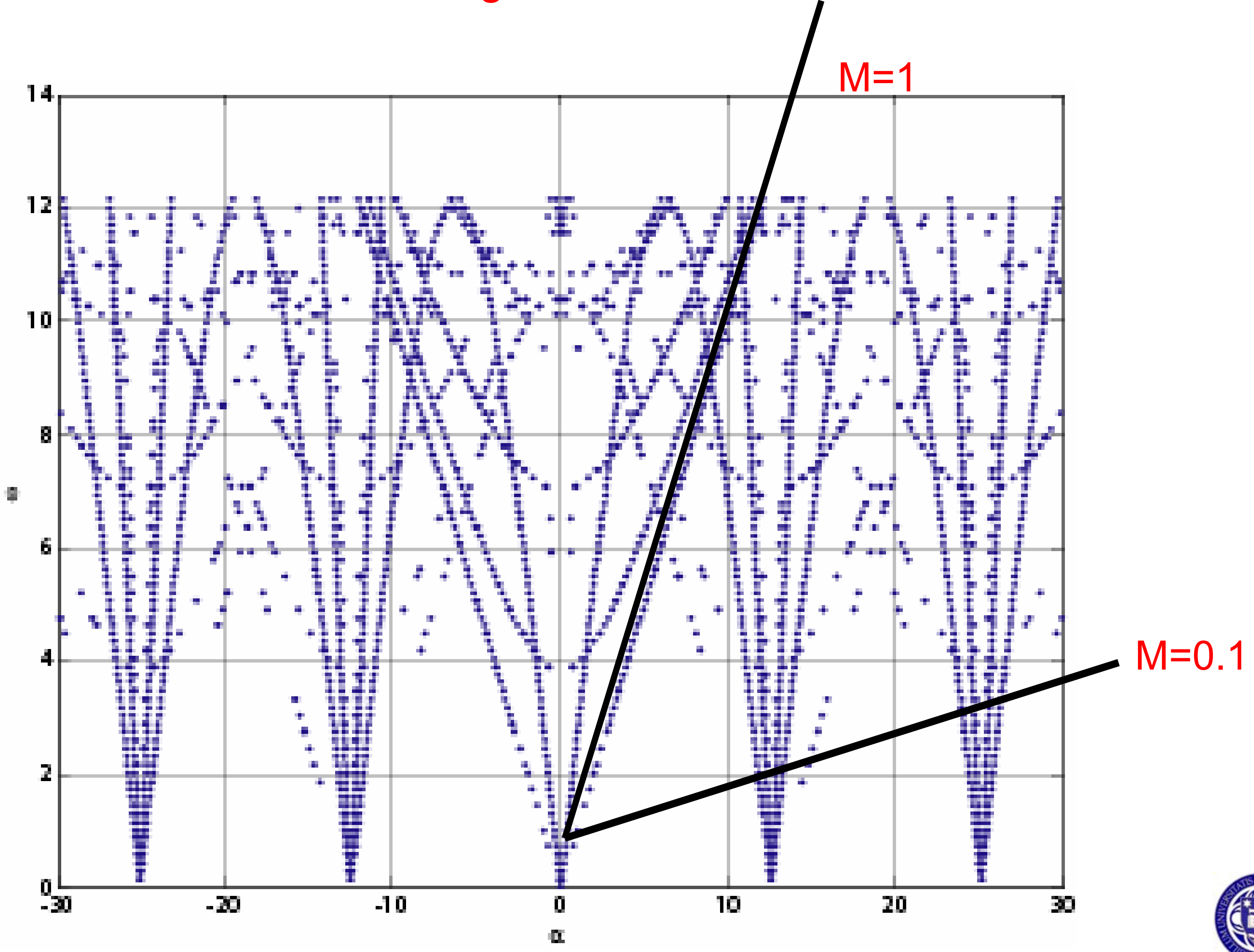

Pressure Directivity of a Monopole and a Dipole in a Submerged Water-filled Elastic Steel Duct

The duct has a radius a= 1 m and thickness h= 0.01m. The unit strength monopole is located along the duct axis. The reduced frequency $\omega^*=a\,\omega/c0=0.5$

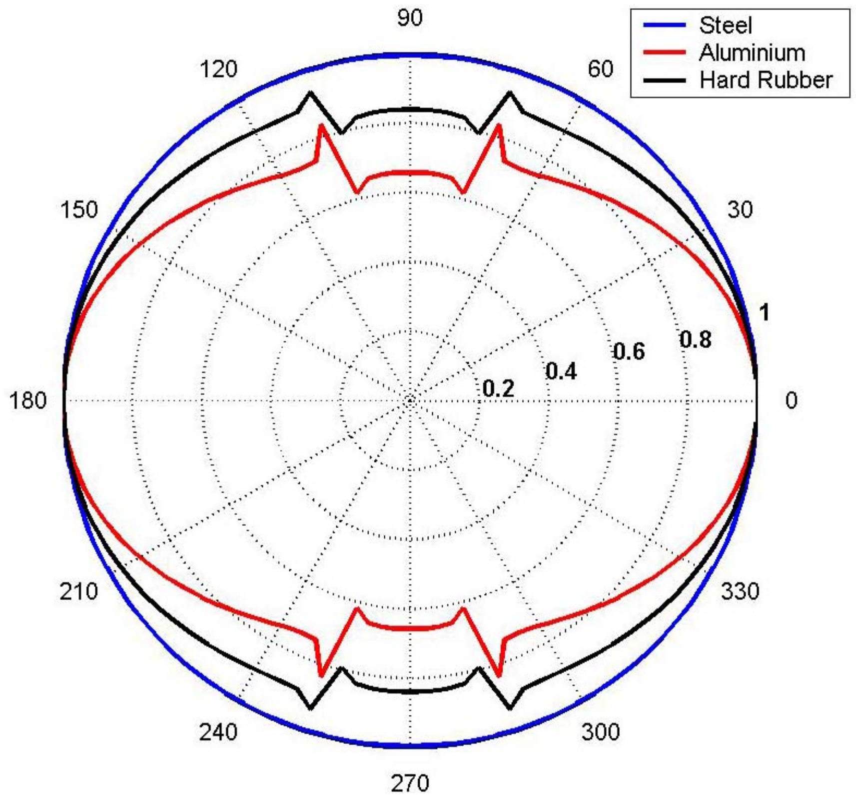

Monopole

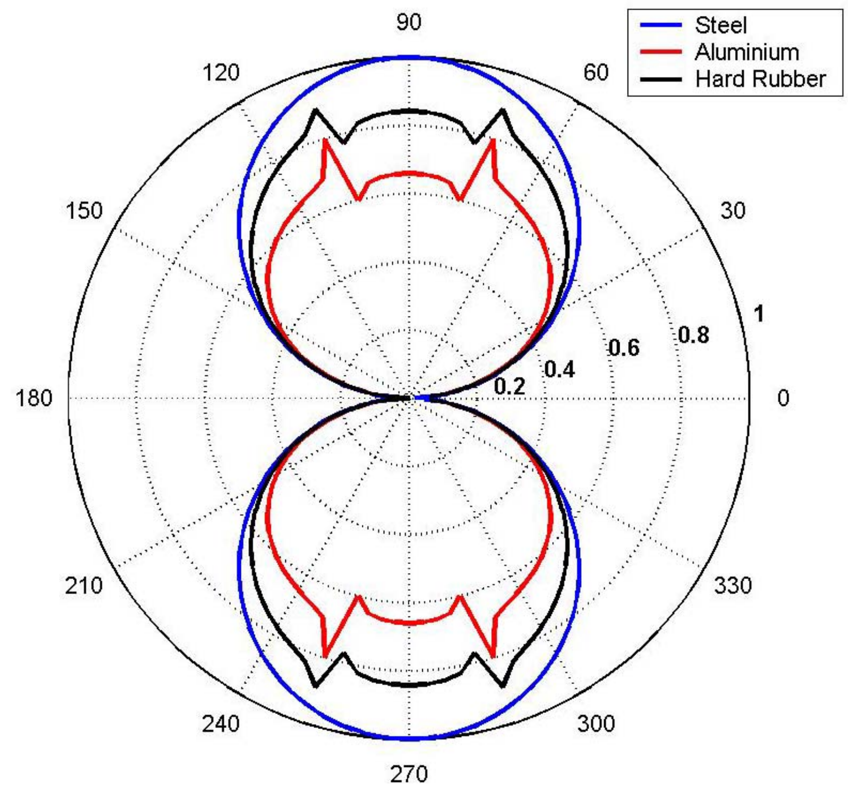

Dipole

Effect of Elastic Wall on the Blade Unsteady Lift

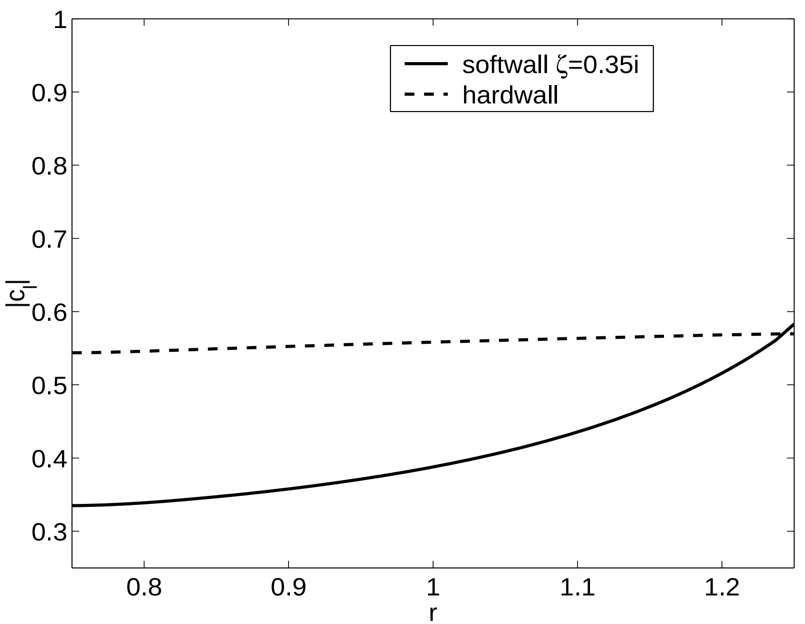

Impedance ς=0.35i

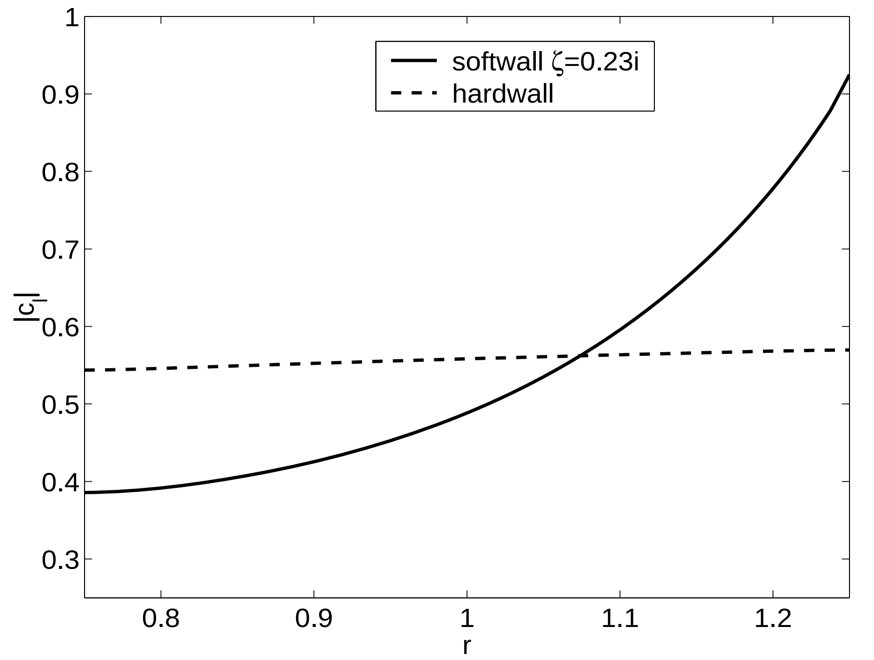

Impedance ς=0.23i

Summary of analysis

- Elastic wall can significantly affect the strength and location of dipole sources.
- Hydrodynamic disturbances may couple with ribbed duct modes producing dipole strength sources
- Ribs change dispersive relation and make it possible for waves with wave length of the order of the duct radius to propagate.
- Comparison with experimental results is planned.

Conclusions

- Analytical and computational analyses yield efficient tools to model acoustically relevant fluid-structure interaction problems characterized by high frequency, complex geometry and coupling with duct modes.
- Important physical features governing these phenomena are outlined and quantified. Results can be used in engine and propeller design to reduce noise.